Supplementary Information

Parallel transmission in a synthetic nerve

Charlotte E.G Hoskin, Vanessa Restrepo Schild, Javier Vinals Camallonga, Hagan Bayley

Supplementary Information: Contents

Supplementary Information: Materials and Methods

Chambers.

Droplet pair chamber. For electrical recordings, a bespoke cuboidal chamber (poly(methyl methacrylate), PMMA) with external dimensions of 10 mm x 10 mm x 6 mm, and internal dimensions of 8 mm x 8 mm x 5 mm, was designed using AutoCAD software (SolidWorks) (Fig. S24a). For optical experiments, a bespoke chamber (PMMA, 20 mm x 20 mm x 6 mm) containing 16 wells (diameter 1.5 mm, height 5 mm) was designed using AutoCAD software (SolidWorks) (Fig. S24b). Chambers have a 1-mm thick base for imaging. The chambers were manufactured by micromilling of PMMA with a Roland Modela MDX-40A computerized numerical control (CNC) machine. At the start and end of each experiment all chambers were washed twice with water and ethanol and dried using a nitrogen gas stream.

Synthetic neuron chamber. Bespoke chambers for the synthetic neurons were designed using AutoCAD software (SolidWorks, Fig. S24c-d). For straight synthetic neurons, a chamber was built with outer dimensions of 15 mm x 10 mm x 6 mm and four cuboidal trenches with dimensions of 10 mm x 1 mm x 5 mm (Fig. S24c). For the curvy neuron experiments a cuboidal chamber was designed with outer dimensions of 30 mm x 20 mm x 5 mm, and inner dimensions of 26 mm x 16 mm x 3 mm (Fig. S24d). The neuron-shaped trench was then hand-drawn using AutoCAD; the depth was 1 mm, and the diameter ~ 1 mm (varied as hand-drawn). The neuron diameter (~ 1 mm) was comparable to the diameter of the giant squid axon (*Architeuthis dux*, 0.5 - 1.5 mm). As described above, a CNC machine was used to manufacture the chamber (Fig. S24d).

Synthetic nerve chamber. Bespoke chambers for the synthetic nerve were designed using AutoCAD software (SolidWorks). A cuboidal PMMA chamber was used with outer dimensions of 30 mm x 30 mm x 30 mm and inner dimensions of 24 mm x 24 mm x 29 mm (Fig. S24e). As described above, a CNC machine was used to manufacture the chamber.

Synthetic nerve cast. Bespoke casts were designed using AutoCAD software (SolidWorks, Fig. S23e). The casts were manufactured using Low Force Stereolithography Form 3 (FormLabs) with Clear Resin (FormLabs) and were subsequently washed with Form Wash (FormLabs) before curing with Form Cure (FormLabs). The nerve cast had outer dimensions of 25 mm x 25 mm x 15 mm and inner dimensions of 16.65 mm x 15 mm x 10 mm (Fig. S24f). Within the nerve cast were seven cylindrical tubes (diameter 1 mm and height 10 mm) spaced with their centres 4 mm apart (Fig. S24f). Prior to use, all casts were washed with water and ethanol and dried using a nitrogen stream.

Preparation of materials.

Aqueous solutions. Solution A contained 100 mM MES (Sigma, M3671) and 100 mM sodium chloride (NaCl, Sigma, S7653), 0.001% DDM (w/v), pH 6.5. Solution B Solution A contained 100 mM MES (Sigma, M3671) and 100 mM sodium chloride (NaCl, Sigma, S7653), pH 6.5. Solution C contained 100 mM NaCl (Sigma, S7653), pH 6.5. All solutions were filtered using 0.22 μm Millex GP filters (Millipore) before use.

Lipid-in-oil preparation. 1,2-Diphytanoyl-sn-glycero-phosphatidylcholine (DPhPC, Avanti, 4ME, 16:0 PC, 850356P) was dissolved in chloroform, aliquoted into glass vials (7 mL, Supelco) and dried with a stream of nitrogen gas to form a lipid film. The film was placed in a vacuum for 3 h and then dissolved at the requisite concentration in filtered (0.22 μm Millex GP

filters, Millipore) hexadecane (Sigma, H0255) and silicone oil (AR20, Sigma, 10836) (35:65 (v/v)) and stored at room temperature.

Microbial rhodopsin preparation. Light-activated rhodopsins were gifts from the Watts Group, Department of Biochemistry, University of Oxford. The experiments displayed in this paper used proteins from 13 different batches (prepared between 2016 - 2020 but following the same protocol); each experiment used light-driven protein from a single batch.

Archaerhodopsin-3 (aR3) was expressed in its native archaea *Halorubrum sodomense* (strain RD-26, LGC Standards Ltd) and purified as fragments of the claret membrane (CM) (as confirmed by AFM[1]). Samples were stored at 4°C in the dark. Prior to use the buffer in each protein sample was exchanged into Solution A by using a P6 BioSpin column (BioRad, 7326227). The sample was then sonicated, in a bath, for 30 min at 20°C (Branson 2800, Cleanosonic) before dilution with Solution B to a final concentration of 0.001% DDM and 0.15 - 0.25 mg protein mL^{-1} (estimated from measurements taken with a Nanodrop 1000 Spectrophotometer). Before each experiment, the protein was gently vortexed to reduce protein aggregation.

Archaerhodopsin-3 (aR3) was also expressed in *Escherichia coli* (EC), purified, and confirmed to be the monomer by a hypsochromic shift in absorbance[2]. The template plasmid was WT Arch-3 in pET28b [addgene ID: 58487]. The plasmid encoded an oligoHis tag (His6) at the C-terminal end of the aR3 gene. After purification, the EC-aR3 protein was reconstituted using detergent into vesicles and stored at 4°C in the dark. Prior to use, EC-aR3 samples were prepared as described for CM-aR3 (buffer exchanged, sonicated in a bath, and diluted) with a final protein concentration of 0.15 - 0.25 mg mL^{-1} (estimated from measurements taken with a Nanodrop 1000 Spectrophotometer). Before each experiment, the protein was gently sonicated (30 min at 20°C) and vortexed to reduce protein aggregation.

Bacteriorhodopsin (bR) was expressed in its native archaea *Halobacterium salinarum* and purified as fragments of the purple membrane (PM)[1-3]. Protein samples were stored at 4°C in the dark. Prior to use, protein samples were treated as described for CM-aR3 (buffer exchanged, sonicated in a bath, and diluted) with a final PM-bR concentration of 0.15 - 0.25 mg protein mL^{-1} (estimated from measurements taken with a Nanodrop 1000 Spectrophotometer). Before each experiment, the protein was gently sonicated (in a bath for 30 min at 20°C) and vortexed to reduce protein aggregation.

Alpha hemolysin preparation. The pore-forming protein, alpha hemolysin (αHL), was kindly provided by Idil Cazimoglu (Bayley Group). The protein was expressed in the bacteria *Escherichia coli* (Agilent) using the αHL-D8H8 plasmid, purified as monomers (as confirmed by SDS-PAGE electrophoresis) and stored at -80°C. Before use, protein samples were exchanged into Solution A to a final concentration of 50 nM. A fresh aliquot was prepared for each experiment.

Pyranine solution. Pyranine dye (8-hydroxypyrene-1,3,6-trisulfonic acid, HPTS, H1529, ThermoFisher) was dissolved in Solution B at 100 μM and stored at 4°C in the dark. When required, CM-aR3 was exchanged into the pyranine solution by using a P6 BioSpin column (BioRad, 7326227) to give a final concentration of 0.15 – 0.25 mg mL^{-1} CM-aR3 in Solution B containing 100 μM pyranine and 0.001% DDM (w/v). All experiments with pyranine were performed in the absence of MES buffer to produce measurable changes in droplet pH.

Hydrogel axon preparation. Agarose (2% high-gelling agarose, Sigma, A9045) was dissolved in Solution A and stored at room temperature. Prior to use, the hydrogel was heated to 95°C in a dry block heater to enable pipetting.

MANT-dATP solution. MANT-dATP (3'-O-(N-methylanthraniloyl)-2'-deoxyadenosine 5'-triphosphate triethylammonium salt, Sigma, 69258) was dissolved at 100 μM in Solution A containing 50 nM αHL and stored at -20°C in the dark.

ATP-dependent reaction kit preparation. ATP (adenosine 5′-triphosphate, Sigma, A2383) was dissolved at 100 μM in Solution A containing αHL (50 nM) and stored at -20°C. The remaining components of the ATP-dependent reaction kit (Abcam, ab83355) were prepared and stored according to the manufacturer's manual.

Elastomer nerve preparation. Silicone elastomer monomer (SYLGARD 184, Sigma, 761036) and curing agent (Sigma, 761036) were mixed in a 10:1 (v/v) ratio and degassed for 30 minutes. The mixture was then poured into a bespoke cast (Fig. S23f), avoiding the formation of bubbles. The filled cast was placed in an incubator overnight at 60°C. After the elastomer had cooled, it was cut at the edges of the cast using a scalpel. Silicone oil (AR20, Sigma, 10836) was then pipetted down the interface between elastomer and cast. After 24 h, this elastomer nerve was carefully removed from the cast with a spatula and tweezers.

Construction of the synthetic tissues.

Synthetic neuron. All synthetic droplet neurons were composed of a series of aqueous droplets (200 nL, ~700 μm diameter) connected through droplet interface bilayers (DIBs). The sensory bilayer was composed of a DIB formed between a CM-aR3 sensory droplet (0.15 – 0.25 mg mL^{-1} CM-aR3, 0.001% DDM, Solution A) and a protein-free droplet (Solution A). All subsequent droplets in the axon contained αHL protein (50 nM αHL in Solution A). At the other end of the droplet axon were two additional aqueous droplets, the presynaptic and postsynaptic droplets (Fig. 1c). The presynaptic droplet contained αHL (50 nM αHL in Solution A), and the small molecule neurotransmitter MANT-dATP (a fluorescent analogue of ATP). This droplet formed one bilayer with the axon and another with the protein-free postsynaptic droplet (Solution A), here referred to as the synaptic bilayer. During construction, all droplets were incubated in lipid-in-oil for 5 minutes to enable monolayer formation. Next, the sensory and synaptic bilayers were formed by gently pushing the droplets together using a silver wire or tipping the chamber. In the case of tethered synthetic neurons (Fig. S12-13), the terminal neuron droplets were placed directly onto the electrodes and the micromanipulators used for droplet movement. Finally (after a further 5 minutes), the axon droplets were connected (in the same manner) to complete the synthetic neuron. After bilayer formation, protein inserted into the new interfaces. All synthetic hydrogel neurons were composed of a hydrogel axon (2% high-gelling agarose, Solution A) connected to aqueous droplets (200 nL, ~700 μm diameter) via droplet hydrogel bilayers (DHBs). First, the hydrogel axon was built by pipetting hot agarose into the chamber. Next, lipid-in-oil was added to the chamber. Droplets were pipetted at either end of the axon and, after 10 minutes incubation, the sensory and synaptic bilayers were formed. Here, the sensory bilayer was composed of a DHB formed between a CM-aR3 sensory droplet (0.15 – 0.25 mg mL^{-1} CM-aR3, 0.001% DDM, Solution A) and a protein-free hydrogel axon. After a further 10 minutes, the presynaptic droplet was connected to the hydrogel axon to complete the synthetic neuron. Synthetic neuron formation was performed in a dimly lit room.

Neighbouring droplet. A tetherless synthetic droplet or hydrogel neuron was built as described above; here ATP (not MANT-dATP) was added to the presynaptic droplets. The synthetic neuron was then illuminated overnight (15 h, YG light, 15 ± 4.5 mW). A neighbouring droplet (200 nL) containing the ATP-dependent reaction kit (ATP Assay kit, Abcam, ab83355) was pipetted at the synaptic end of the synthetic neuron. Using a piece of silver wire (100-μm diameter, Sigma, 348783), the postsynaptic droplet was carefully separated from the presynaptic droplet. The postsynaptic and neighbouring droplets were then fused; this happened readily since the neighbouring droplet contained glycerol which destabilised the

bilayer. After 30 minutes in the dark (in a hydration chamber), during which the ATP-dependent reaction occurred, the fused droplets (400 nL) were gently brought into contact with the presynaptic droplet to recomplete the synthetic neuron (Fig. S21-22).

Insulated synthetic neuron. Silicone elastomer monomer (SYLGARD 184, Sigma, 761036) and curing agent (Sigma, 761036) were mixed in a 10:1 ratio and degassed for 30 minutes. The mixture was then poured into a cylindrical cast, made from a piece of PVC plastic tubing (length 10 mm, diameter 5 mm) glued at one end onto a PMMA block; a central glass rod (length 10 mm, diameter 1 mm) was glued in the centre. Care was made to avoid the formation of bubbles. The filled cast was placed in an incubator overnight at 60°C. Once cooled, the PVC plastic tubing was cut with a scalpel and the elastomeric sheath removed from the cast. The central tube was then removed using tweezers and the tubular hole filled with hot hydrogel (2% high-gelling agarose) to form the axon. The insulated synthetic neuron was then composed of a central hydrogel axon within an elastomer sheath (Fig. 1d, S23). Once the hydrogel had cooled, the neuron was transferred into a large chamber (5-cm square, PMMA) containing lipid-in-oil for electrical recording. Droplets (200 nL) were first incubated in a separate chamber containing lipid-in-oil and after 5 - 30 minutes pipetted into the neuron chamber. For tethered neurons, the droplets were placed directly onto the electrodes and the micromanipulators used for droplet movement.

Synthetic nerve. The elastomeric nerve structure was removed from the cast leaving seven tubular holes within it (where the seven rods, with dimensions of 1 mm diameter and 10 mm length, were positioned) (Fig. S24f). These holes were filled by pipetting hot hydrogel (2% low-melt agarose, Sigma) into them, thereby forming the axons. The hydrogel axons fitted tightly into the elastomer sheath, but they were not fixed to it thereby permitting damaged ones to be carefully removed with tweezers and replaced. The synthetic nerve was composed of seven conducting hydrogel axons within the elastomeric nerve casing. Finally, droplets were added at each end of the hydrogel axons.

Electrical recordings.

Electrical recording and analysis. For tethered synthetic neurons and nerves, signals were recorded with an amplifier (Axopatch 200B, Axon Instruments), connected to a digitizer (Digidata 1440 A, Axon Instruments), operating in gap-free acquisition mode at a sampling frequency of 10 kHz, with a 2 kHz filter and five-fold gain. Data was analysed with Clampfit (version 10.3, Axon Instruments) after post-filtering with a 25 Hz low-pass filter. Electrical recordings were conducted at 24.5 $\pm$ 3.4°C and 32.4 $\pm$ 8.6% humidity. Temperature (20 - 29°C) and humidity (20 - 50%) fluctuated and extreme values led to difficulties in forming stable bilayers because frequency of droplet coalescence increased. Under sub-optimal environmental conditions, monolayer incubation times were increased to at least 30 minutes to improve stability.

Electrode preparation. Ag/AgCl electrodes were prepared by soldering silver wire (100-μm diameter, Sigma, 348783) into male crimp-terminals (RS Components) The wire tips were incubated in sodium hypochlorite (NaClO, 10% active chlorine, Sigma, 28-3100) for a few minutes and then their surfaces were coated with a hydrogel layer by pipetting hot melted agarose (1% low-melt agarose, Sigma, A9045). Electrodes were stored at room temperature in the dark. The male crimp-terminals of these electrodes were each plugged into a female crimp-terminal (RS Components), which was in turn attached to a micromanipulator (Narishige, NMN-21). The other end of the female crimp-terminal was soldered to a cable terminating in a second male crimp-terminal. These second male crimp-terminals were connected to the amplifier headstage (Axopatch 200B, Axon Instruments), one at the grounding site and one at the recording site.

Illumination source. Fibre-coupled LEDs were used as an illumination source (Mightex, WFC-H7-0560). The LED bundle was composed of 7 distinct LEDs, each of which is controlled by a separate channel using the manufacturer's software (Mightex): LED channel 1 (680 - 741 nm peaks at 722 nm), 2 (634 - 680 nm peaks at 660 nm), 3 (603 - 645 nm peaks at 631 nm), 4 (576 - 608 nm peaks at 592 nm), 5 (490 - 594 nm peaks at 550 nm), 6 (392 - 430 nm peaks at 410 nm), 7 (355 - 390 nm peaks at 367 nm) (Fig. S6). The LED bundle was passed through a hole at the top of the Faraday cage (solid metal, Fig S7a) via a bespoke adaptor (Mechanical Workshop, University of Oxford) and aligned to the PMMA neuron chamber at a distance of 5 cm (Fig. S7a). All microbial rhodopsins were illuminated with yellow-green (YG) light (channels 4 and 5 simultaneously, 490 - 608 nm peaks at 592 nm and 550 nm) unless otherwise stated. Spectral information for all LED channels was obtained using an Optical Spectrum Analyser (Thorlabs) with the LEDs run at 10 mA (all LED channels on) and at the maximum intensity for each channel (single LED channel on) (n = 3 traces) (Fig. S6).

Electrode controls. Electrode controls were performed at the start and end of an experiment to ensure no artefacts arose from photochemistry at the Ag/AgCl electrode surface. Two protein-free aqueous droplets (200 nL, Solution A) were pipetted onto the electrodes. After a 5-minute incubation period, the droplets were brought into contact with the micromanipulators and spontaneously formed a droplet interface bilayer (DIB). First, a capacitance measurement (determined by applying a triangular voltage waveform, $\pm$ 15 mV, 30 s peak-to-peak) was made in the dark to determine if a DIB had formed. It was assumed that bilayer formation had occurred if the capacitance was >20 pF. Higher capacitance was indicative of a larger bilayer area. Then, the droplet pair was illuminated, first with IR light (LED channel 1, 680 - 741 nm, peak at 722 nm, 16 $\pm$ 5.0 mW), or with UV light (355 - 390 nm, peak at 367 nm, 15 $\pm$ 3.9 mW), and then with YG light (channels 4 and 5, 490 - 608 nm, peaks at 592 nm and 550 nm, 15 $\pm$ 4.5 mW) (Fig. S6). Electrodes that generated a signal when illuminated were discarded and fresh electrodes made.

Tethered droplet pairs set-up. Electrical recordings were performed within a Faraday cage containing 1. A platform (Mechanical workshop, University of Oxford) supporting the headstage of a conventional patch-clamp amplifier (Axopatch 200B, Axon Instruments); 2. Two micromanipulators (Narishige, NMN-21) to move the electrodes; and 3. The experimental PMMA chamber. The chamber was filled with lipid-in-oil and placed at the centre of the platform directly under the LED fibre bundle (Fig. S7a). The electrodes were observed with a stereomicroscope (Nikon, SMZ660) and positioned with the micromanipulators so that their terminals were immersed in the lipid-in-oil. Droplets (200 nL) were pipetted onto each electrode (Finnpipette F1, 0.2-2 μL, ThermoFisher). The droplets hung on the electrode tips, adhering to the hydrogel coating. The sensory droplets (containing the CM-aR3 protein) were placed on a recording electrode, and the ground electrode was within a droplet containing only Solution A. After incubation for 5 min, the two droplets were gently brought into contact (using the micromanipulators) when a DIB spontaneously formed, as confirmed by measurement of the capacitance (>20 pF) (Fig. S7a). The capacitance values of the protein-containing bilayers were lower than those for bilayers that did not contain protein, indicative of smaller bilayers.

Sensory droplet activity. Droplet pairs containing one sensory droplet (with the recording electrode) and one protein-free droplet (Solution A, with the ground electrode) were illuminated with IR light (680 - 741 nm, peak at 722 nm, 16 $\pm$ 5.0 mW), or with UV light (355 - 390 nm, peaks at 367 nm, 15 $\pm$ 3.9 mW) (Fig. S6). If a signal was observed, the experiment was abandoned since neither UV nor IR light can activate the microbial rhodopsins used in this paper (Fig. S4, S27). If no signal was observed, then the droplet pair was illuminated with YG light (490 – 608 nm, peaks at 550 nm and 592 nm, 15 $\pm$ 4.5 mW) (Fig. S6). LED output was measured using a compact power meter console ThorLabs. Sensory droplets containing active protein, generated signals greater than 2.0 pA (an arbitrary threshold set to indicate activity). The maximum signal detected was +25 pA (+19 $\pm$ 3.9 pA, mean $\pm$ SD, n = 10 droplet

pairs, Fig 2). Alongside illumination with IR and UV light, control experiments were performed in the absence of light (D, Dark) and absence of CM-aR3 protein (NP) to confirm that the light-driven H^+ pumping of CM-aR3 (under YG illumination) was responsible for the outputs observed.

Action spectra. A droplet pair was prepared as described above with the recording Ag/AgCl electrode in a sensory droplet (+ CM-aR3, 200 nL) and the ground electrode in a protein-free droplet (Solution A only, 200 nL). The droplet pair was then illuminated using a fibre-coupled LED bundle, composed of 7 distinct LEDs, each of which was controlled as a separate channel using the manufacturer's software (Mightex): LED channel 1 (680 - 741 nm peaks at 722 nm), 2 (634 - 680 nm peaks at 660 nm), 3 (603 - 645 nm peaks at 631 nm), 4 (576 - 608 nm peaks at 592 nm), 5 (490 - 594 nm peaks at 550 nm), 6 (392 - 430 nm peaks at 410 nm), 7 (355 - 390 nm peaks at 367 nm) (Fig. S6). First, the signal output was recorded upon illumination with YG light (Channels 4 + 5 simultaneously, 490 – 608 nm with peaks at 550 nm and 592 nm, 15 $\pm$ 4.5 mW (measured by a compact power meter console ThorLabs)) as described above. This was also performed at the end of each experiment to ensure protein activity was maintained. The LED fibre bundle, inserted into the Faraday cage through an adaptor (Mechanical workshop, University of Oxford), was then connected to a second adapter (SM1A1, ThorLabs) on the inside of the Faraday cage. Bandpass filters were screwed into the second adapter at a distance of 4 cm from the PMMA chamber containing the DIB. These filters allowed light of a narrow wavelength band to pass ($\pm$ 10 nm). In turn, filters allowing light at 390 nm, 430 nm, 490 nm, 530 nm, 560 nm, 590 nm, 630 nm and 660 nm were fitted. All LED channels were run at 0.2 $\pm$ 0.1 mW output (measured by a compact power meter console ThorLabs). The illumination protocol was controlled from a computer by using the manufacturer's software (Mightex). Electrical traces were recorded for each filter as described above, using Clampex, and analysed using Clampfit (version 10.3, Axon Instruments). If the droplet pair coalesced, then the experiment was stopped and restarted.

Tethered synthetic neuron set-up. Electrical recordings were performed within a Faraday cage, as with 'Droplet pairs'. The bespoke neuron chamber was placed in the centre of the stage. For the tethered droplet-based neurons, the chamber was first filled with lipid-in-oil. All droplets (200 nL) were first incubated after pipetting into a separate container. After 5 - 30 minutes, the droplets were transferred by pipette into the trench of the neuron chamber (Fig. S31). The recording electrode was inserted into the sensory droplet and the ground electrode into the terminal synaptic droplet. These droplets were moved using the micromanipulators. The central droplets were positioned by hand using a piece of silver wire (100-μm diameter, Sigma, 348783). When two droplets were brought into contact a DIB spontaneously formed. For the hydrogel-based neurons, 'stoppers' (handmade from pipette tips) were positioned at the terminals of the trench. The hot hydrogel (prepared as described above) was then pipetted into the trench of the chamber and left to cool. Once cooled, the 'stoppers' were removed and the chamber was filled with lipid-in-oil, coating the hydrogel. The chamber was then placed in the centre of the stage within the Faraday cage. Droplets were incubated in a separate array and after 5 - 30 minutes they were transferred by pipetting to the appropriate sites on the neuron. They were then gently pushed into contact with the hydrogel axon by tipping the chamber, forming droplet hydrogel bilayers (DHBs). Once all bilayers had formed electrical recordings were made as described for the 'Sensory droplet activity'.

Simultaneous recording in tethered synthetic nerves. The synthetic nerve-containing chamber (Fig. S24, S25) was filled with lipid-in-oil and placed in the centre of the stage directly under the LED bundle, inside the first of two Faraday cages. The sensory end of the nerve was surrounded with light-blocking sheets (made from waterproof black card) to permit independent stimulation of neighbouring axons (Fig. S25). Electrical recordings were conducted with a multichannel amplifier (Triton$^+$, Tecella LLC), which was placed in a second Faraday cage adjacent to the first (Fig. S25). Hydrogel-coated Ag/AgCl electrodes (prepared as described above) were connected to the amplifier through an 8-channel electrode probe

holder (Terrapin, Tecella LLC) with each channel ending in a screw-terminal. Each electrode was connected to the screw terminals to enable individual recording from each electrode. The probe holder was contained within an aluminium box within the first Faraday cage (Fig. S25). With the aid of a stereomicroscope, electrodes were carefully positioned within 0.5 mm of the hydrogel axons. Aqueous droplets (200 nL) were pipetted directly onto the electrodes, following a 5 - 30-minute incubation in a separate PMMA chamber, forming DHBs with the hydrogel axons. Each axon was illuminated using a distinct fibre-coupled LED (490 - 608 nm, peaking at 560 nm, 15.0 $\pm$ 4.5 mW (measured by a compact power meter console ThorLabs), Mightex, WFC-H7-0560) (Fig. S6). The LEDs were positioned within the first Faraday cage (Fig. S25) using separate clamp-stands. The LED of Axon 1 was controlled from a computer with the manufacture's software (Mightex) by using the strobe setting with 15 s light pulses (at 0.05 Hz). The LEDs of Axons 2 and 3 were controlled from separate waveform generators (Rigol, DG822) with light pulses of length 1 s and 20 ms at 0.1 and 0.06 Hz respectively. The signal was obtained by gap-free acquisition with a feedback resistor of 1 GΩ. Data was acquired at 20 kHz with a 5 kHz filter with the 'TecellaLab v0.90 type 2′ software. Data from the multichannel amplifier (Triton$^+$, Tecella LLC) was analysed using Clampfit.

Output polarity. To enable signal output to be recorded in 'real' time, tethers (Ag/AgCl electrodes) were added to the droplets; the recording electrode was located within the sensory droplet. When illuminated (YG light), hydrogen ions, (H^+) were injected into the synthetic axon by CM-aR3 pumps generating a positive terminal at the ground electrode and a negative terminal at the recording electrode. Accordingly, negatively charged electrons flowed towards the positive terminal (through the external tethers). This was recorded by the amplifier (Axopatch 200B, Axon Instruments) as a positive signal output (> 0 pA).

Replicates. For all electrical recordings, (a minimum of three) independent synthetic neurons/nerves were built. All sensory droplets were formed using the same aliquot of CM-aR3 protein (0.15 – 0.25 mg mL^{-1} protein, 100 mM MES, 100 mM NaCl, 0.001% DDM, pH 6.5). Likewise, axon (and postsynaptic) droplets were formed using a single solution (100 mM MES, 100 mM NaCl, pH 6.5) and presynaptic droplets were formed using a single solution (50 nM αHL, 100 μM MANT-dATP (or ATP), 100 mM MES, 100 mM NaCl, pH 6.5). Each trace was analysed using Clampfit (version 10.3, Axon Instruments) and the mean steady-state output was plotted as a single data point. All repeats were performed using the same light source (wavelength, intensity etc..) and experimental set-up.

Optical recordings.

Microscope. A Leica DMi8 inverted epi-fluorescence microscope was used for imaging tetherless (in the absence of Ag/AgCl electrodes) synthetic neurons and nerves in brightfield and fluorescence mode.

Illumination protocol. For optical experiments, sensory droplets were illuminated continuously overnight (15 h, YG light); images were taken at 0 h and 15 h. During illumination, the chamber was positioned within a hydration chamber (composed of a petri dish containing multiple water-filled glass vial lids) on the stage and directly below the LED at a distance of 5 cm. The tetherless synthetic neurons and nerves were removed from the hydration chamber for imaging. The same fibre-coupled LED was used as for the electrical experiments, and again controlled by using the manufacturer's software.

Pyranine imaging. Aqueous droplets (200 nL), which contained 100 μM of the pH-sensitive dye pyranine (prepared as described above), were imaged in brightfield and fluorescence mode. The microscope settings used for imaging were: 5 x magnification, with excitation wavelength 450 - 490 nm, emission wavelength 500 - 550 nm, gain 1.0. The fluorescence intensity of pyranine increases with pH[5]. Three images of each droplet were taken (n = 3).

MANT-dATP imaging. Aqueous droplets (200 nL) which contained MANT-dATP, a fluorescent analogue of ATP (Sigma, 100 μM, prepared as described above), were imaged in brightfield and fluorescence mode. The microscope settings used were: 10 x magnification, with excitation wavelength 350-390 nm, emission wavelength 420-480 nm, gain 1.0. Concentrations of MANT-dATP below <18 μM could not be observed. Three images of each droplet were taken (n = 3).

Imaging of downstream signalling. A tetherless synthetic droplet or hydrogel neuron was built as described above; here ATP (not MANT-dATP, 100 μM) and αHL (50 nM) were added to the presynaptic droplets. After illumination (15 h, YG light), the postsynaptic droplet (200 nL) was carefully separated from the presynaptic droplet and fused with the neighbouring droplet (using a piece of silver wire) as described in 'Neighbouring Droplet'. Neighbouring droplets contained an ATP-dependent reaction mix (ATP Assay kit, Abcam, ab83355). After 30 min in the dark (in a hydration chamber), the fused droplets (400 nL) were gently brought into contact with the presynaptic droplet and immediately imaged in brightfield and fluorescence mode (Fig. S21-22). The microscope settings used were: 10 x magnification, with excitation wavelength 540 - 552 nm, emission wavelength 562 - 643 nm, gain 1.0. If ATP was transferred (into the postsynaptic droplet), it phosphorylated glycerol (present in the neighbouring droplet) which was then oxidised to a glycolytic intermediate. Next, the hydrogen peroxide produced in this process generated fluorescent resorufin in another enzymatic conversion (contact Abcam for details). Imaging was immediately after the fused droplet had been reconnected with the presynaptic droplet, because resorufin leaks across droplet bilayers over time, and the high concentration of glycerol destabilises the bilayer causing coalescence of the fused droplet (400 nL) and the presynaptic droplet within 60-120 min. Three images of each droplet (n = 3) were taken.

Image analysis. All fluorescence images were analysed using Fiji (ImageJ). Any brightness or contrast changes made to the images were the same within any image set. In order to determine the fluorescence of a droplet, its cross-section was first plotted, and the mean fluorescence intensity value obtained (mean value of a line scan). Fluorescence analysis of droplets was performed before and after illumination.

Replicates. For all optical experiments, a minimum of three independent synthetic neurons or nerves were built. Each structure was imaged three times and the mean value of a line scan determined using Fiji (ImageJ). The three replicates were averaged to produce a single datapoint. At the start of each experiment, an aliquot of each droplet solution was placed on ice and the same solution used to form all the experimental repeats. These repeats were built and illuminated concurrently, and under the same conditions (e.g., same temperature, humidity, light intensity).

Flexibility experiments.

Bending tubes. Large sheets (length = 20 mm, width = 30 mm, height 10 mm) of hydrogel (2% high gelling agarose in Solution A) or elastomer (Sylgard-184) were made (as described above) and cuboids (length = 20 mm, width = 5 mm, height 5 mm) were cut from them. In addition, a synthetic neuron was formed: a cuboidal elastomer 'sheath' (length = 20 mm, width = 5 mm, height 5 mm) with a central cylindrical hydrogel axon (diameter 1 mm, length 20 mm, with blue food dye for visualisation). Each material was placed over various curved plastic structures, photographed (using an iPhone) and any permanent effect on its structural integrity noted (n = 3 cuboidal structures). The elastomer and synthetic nerve both returned to their original shape after bending. In the case of the hydrogel cuboid, new structures were used (taken from the same larger original sheets) following formation of hydrogel fractures (Fig. S22 b ii). The (cuboidal) synthetic neuron was then placed between the thumb and forefinger and

a video (Supplementary Movie 1) of the material bending was taken, using an iPhone, to demonstrate the synthetic neuron's flexibility.

Display figure preparation.

Brightfield photographs. For display purposes only, brightfield photographs of the neurons and nerves, taken using an iPhone, were processed with the Microsoft background removal feature (Fig. S29). Food dye was added to the droplet and hydrogel components to aid visualisation.

Pyranine microscopy image display. For display purposes only, fluorescence images of the neurons and nerves containing pyranine were background-removed (following stitching if required, see below) (Fig. S30), using Fiji (ImageJ). A mask, formed using the raw data file (Fig. S30b), was superimposed on the raw data file (Fig. S30a). The background (red, BG) was removed, leaving only the fluorescent droplet region (grey). Raw data images were used for image analysis (Fig. S30a) and not the display images (Fig. S30d).

Microscopy image stitching. Overlapping images of the synthetic neurons (containing the fluorescent pyranine dye, MANT-dATP or resorufin) were stitched together using Fiji (ImageJ) pairwise stitching software[6] (Fig. S31). The stitched images were used for display purposes only (Fig. S31d); the raw data images (Fig. S31a) were used for analysis. For MANT-dATP and resorufin experiments, stitched composite images (brightfield and fluorescence channels overlayed) were used; for pyranine experiments only the fluorescence channel was shown.

Supplementary Information: Figures

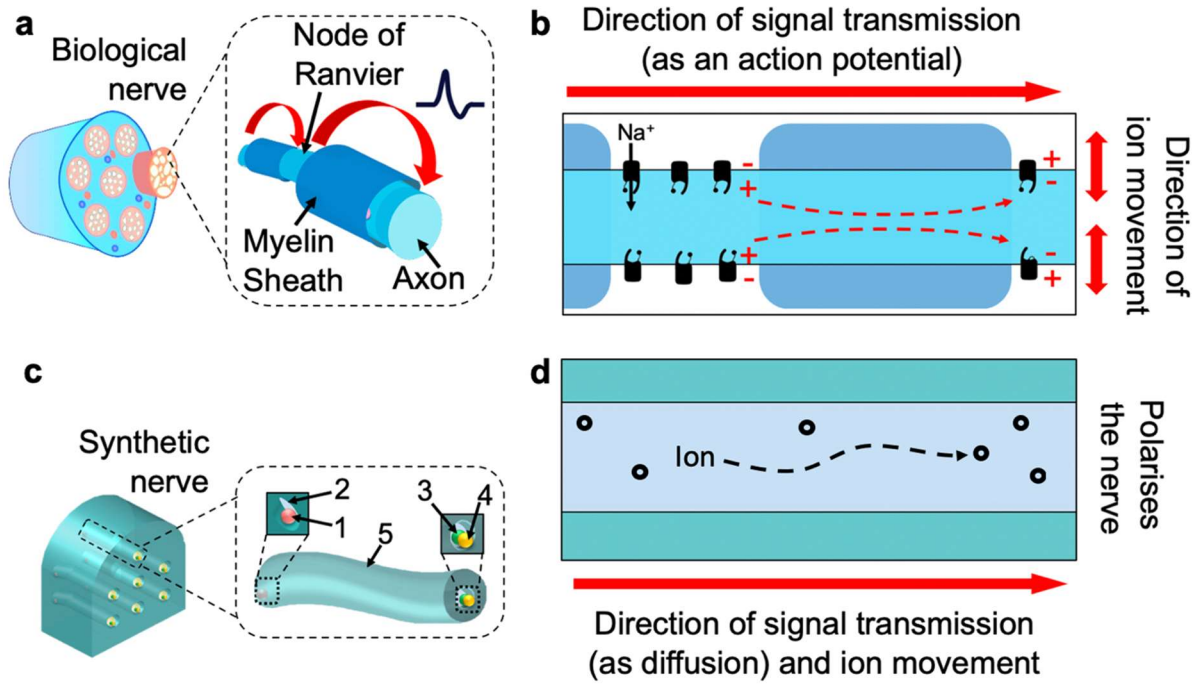

Fig. S1 | Features of a biological neuron. a, Schematic of an afferent biological nerve. Zoom highlights key features of a myelinated neuron: the axon is exposed at Nodes of Ranvier (gaps in the myelin sheath), the action potential propagated by one node of Ranvier jumps to and is regenerated at the next node along the axon, thereby enabling the action potential to travel rapidly along the fibre (red arrow). **b,** Schematic of signal transmission along a biological axon in the form of an action potential[7,8]. Voltage-gated channels (VGCs) mediate ion transport across the axon membrane at the Nodes of Ranvier; the resulting ion gradient polarises the membrane regenerating the action potential. Here, ion movement is perpendicular to the direction of signal transmission. **c,** Schematic of a synthetic afferent nerve. Zoom highlights key features of an insulated synthetic neuron: 1, sensory droplet, 2, hydrogel axon, 3, presynaptic droplet, 4, postsynaptic droplet and 5, insulating elastomer sheath. **b,** Schematic of signal transmission along a synthetic axon in the form of directional ion diffusion. Here both ion movement and signal transmission are in the same direction (i.e., parallel).

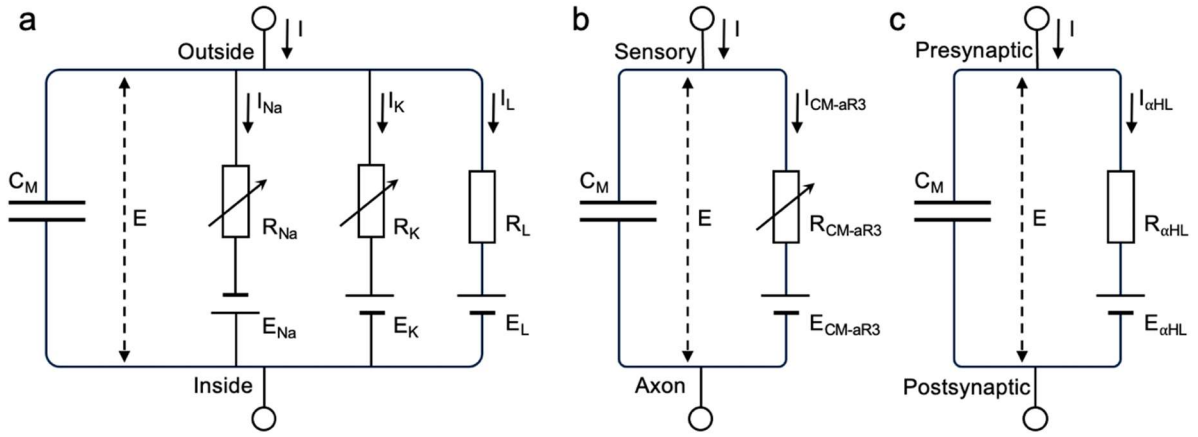

Fig. S2 | Electrical circuit representing an axonal membrane. a, Hodgkin-Huxley model of a biological neuron[9], the membrane is represented by an electrical circuit. The membrane is semipermeable and separates the interior of the cell (inside) from the extracellular fluids (outside) and acts as a capacitor (C_M, describes its ability to store charge). Ionic signals (I) through the membrane can be separated into three components: sodium signal (I_{Na}), potassium signal (I_K) and a small leakage signal (I_L) which arises due to the movement of other ions (mainly chloride ions). Each channel type is represented by a resistor: voltage-dependent sodium (R_{Na}) and potassium (R_K) channels and a small leakage channel (R_L). The arrow indicates that the resistance value is not fixed, varying depending on whether the channel is open or closed. Ion concentrations inside and outside the neuron are unequal and the potential generated by the difference in ion concentration is represented by a battery. Since the potential is different for each ion type, there are separate batteries for the sodium, potassium, and leakage channels, with potentials of E_{Na}, E_K and E_L respectively. **b,** A simple electrical circuit representation of the sensory bilayer. As with the biological neuron, the membrane separates the sensory droplet and axon contents and acts as a capacitor (C_M). Ionic signals (I) through the membrane arise due to hydrogen ion pumping by CM-aR3 (I_{CM-aR3}). The CM-aR3 pumps is represented by a resistor (R_{CM-aR3}) and the arrow indicates that the resistance value is not fixed, varying depending on whether the membrane is illuminated. Ion concentrations on each side of the bilayer are unequal with the potential generated by the difference in ion concentration represented by a battery with potential E_{CM-aR3}. **c,** A simple electrical circuit representation of the synaptic bilayer. As with the biological neuron, the membrane separates the sensory droplet and axon contents and acts as a capacitor (C_M). Ionic signals (I) through the membrane arise due to ion flux through the protein pore alpha hemolysin ($I_{\alpha HL}$). The protein pore is represented by a resistor ($R_{\alpha HL}$). Since ion concentrations on each side of the bilayer are unequal, the potential generated by the difference in ion concentration is represented by a battery ($E_{\alpha HL}$).

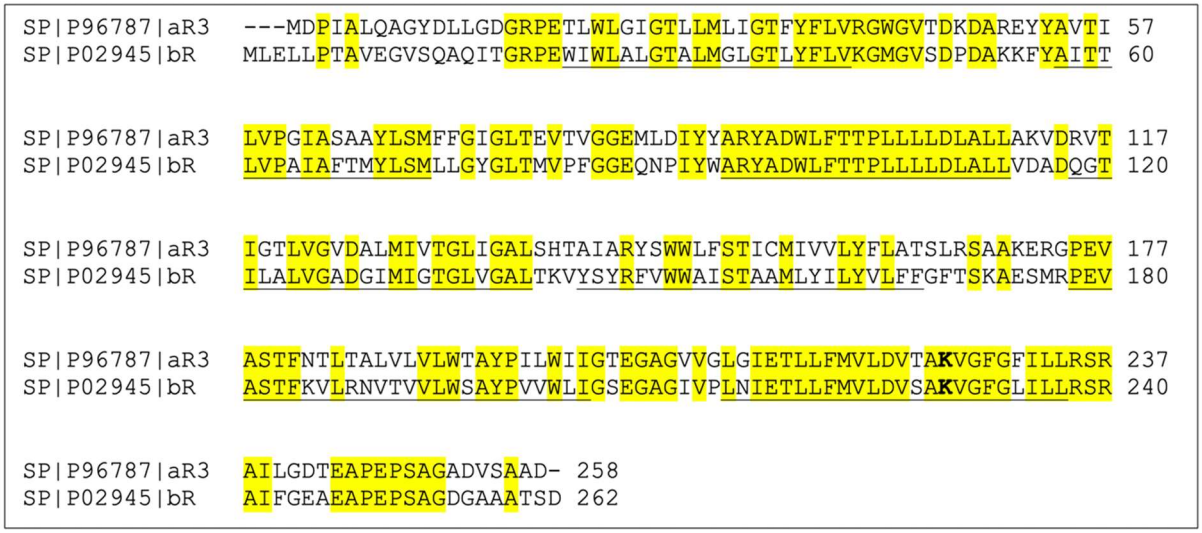

Fig. S3 | Microbial rhodopsin sequence. Alignment of the protein sequences of archaerhodopsin-3 (aR3, P96787) and bacteriorhodopsin (bR, P02945) with the 'Uniprot sequence alignment tool'[10]. Conserved residues are highlighted in yellow, transmembrane regions are underlined and the Schiff base lysine residues are in bold.

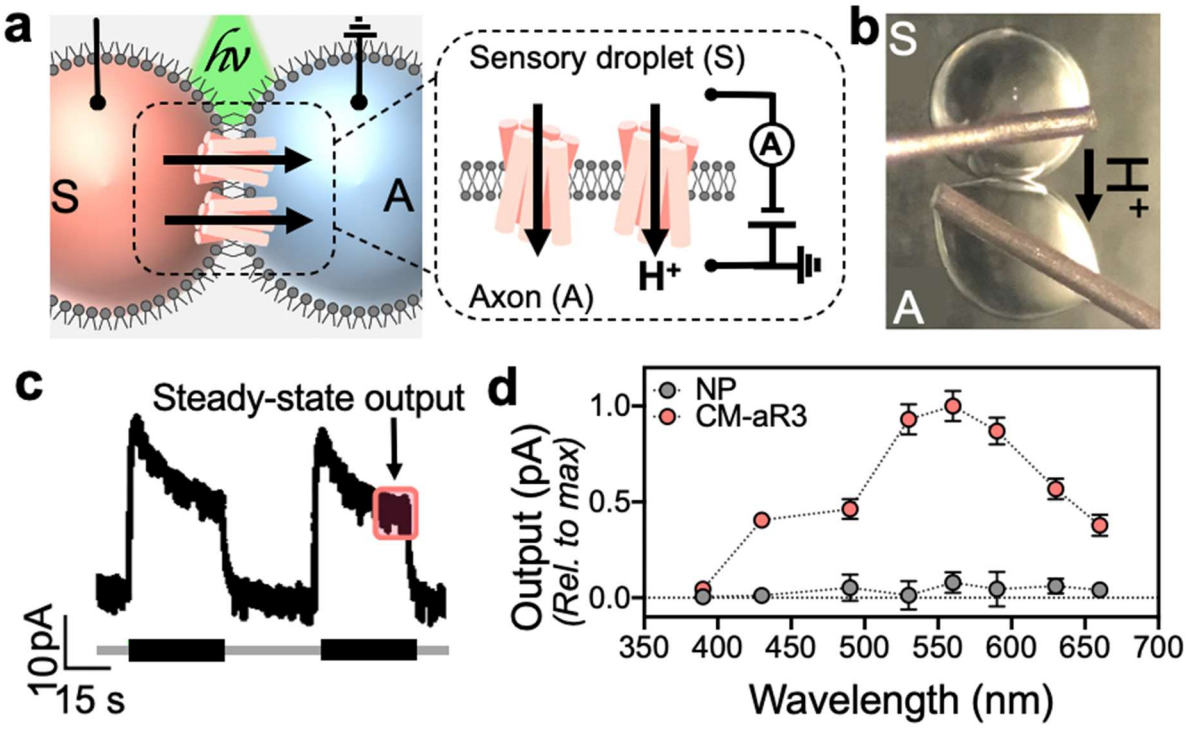

Fig. S4 | Sensory bilayer characteristics. a, Schematic of a droplet pair; the sensory bilayer between the two droplets contains CM-aR3. The recording electrode is inserted into the protein-containing sensory droplet (S, pink). The ground electrode is inserted into the protein-free axon droplet (A, blue). Zoom: illuminated CM-aR3 pumps hydrogen ions (H^+) across the bilayer, and out of the sensory droplet (S) generating a positive signal output (see Materials and Methods). **b,** Photograph of a droplet pair. Hydrogen ions are pumped from the sensory (S) droplet to the axon (A) droplet. **c,** Signal trace recorded when CM-aR3 is illuminated with light (black bars = light on). The steady-state signal is outlined with a box. **d,** Action spectra of sensory bilayers containing CM-aR3 (pink) or no protein (NP, grey). The relative steady-state signal (n = 3 independent DIBs, mean ± SD), when the bilayer is illuminated with light of different wavelengths, is plotted.

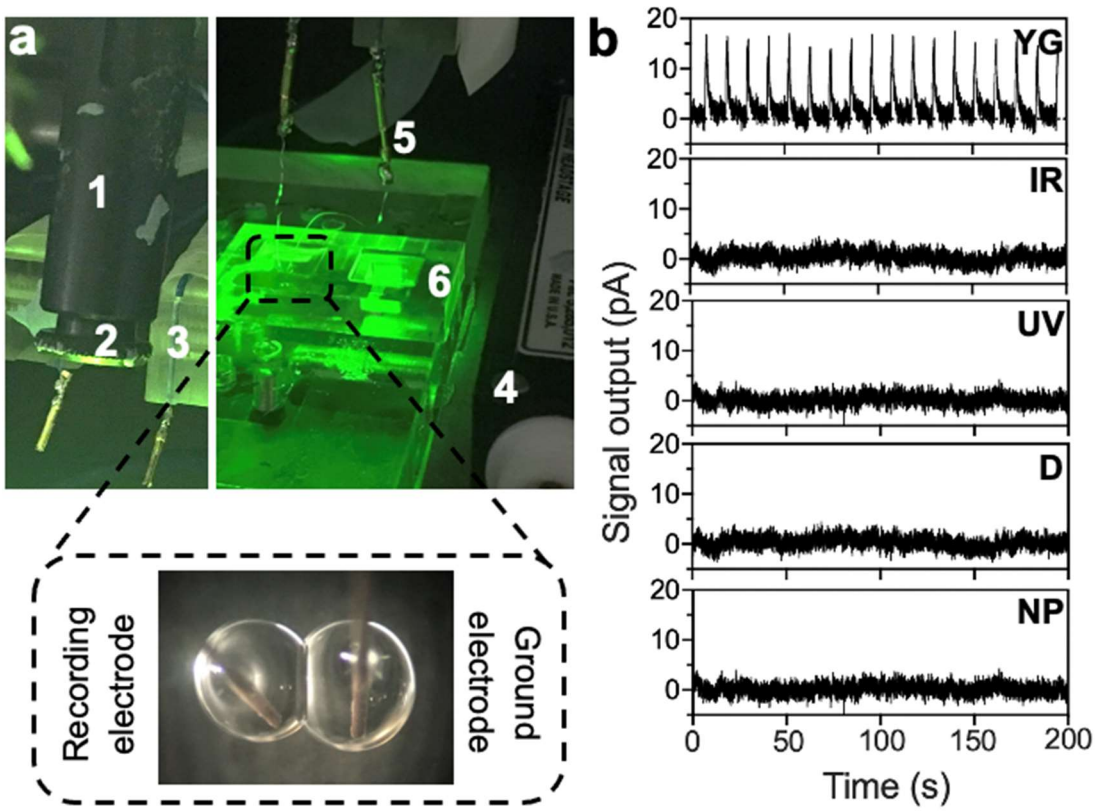

Fig. S5 | Yellow green (YG) light activates CM-aR3. a, Electrical recording from a droplet pair. *Top.* 1. LED holder containing the LED fibre bundle. 2. LED adapter, which holds the LED fibre bundle in place. 3. Holder connecting the electrode to the micromanipulator. 4. Amplifier headstage. 5. Electrodes. 6. Chamber. *Bottom.* DIB set-up with the recording and ground electrodes on either side of the bilayer. **b,** Electrodes record signals generated across the DIB upon illumination (3 s pulses, 0.1 Hz) with YG light, IR light or UV light. Controls were performed in the absence of light (D) and the absence of protein (NP). Light output is 15.0 ± 4.5 mW (n = 1 DIB).

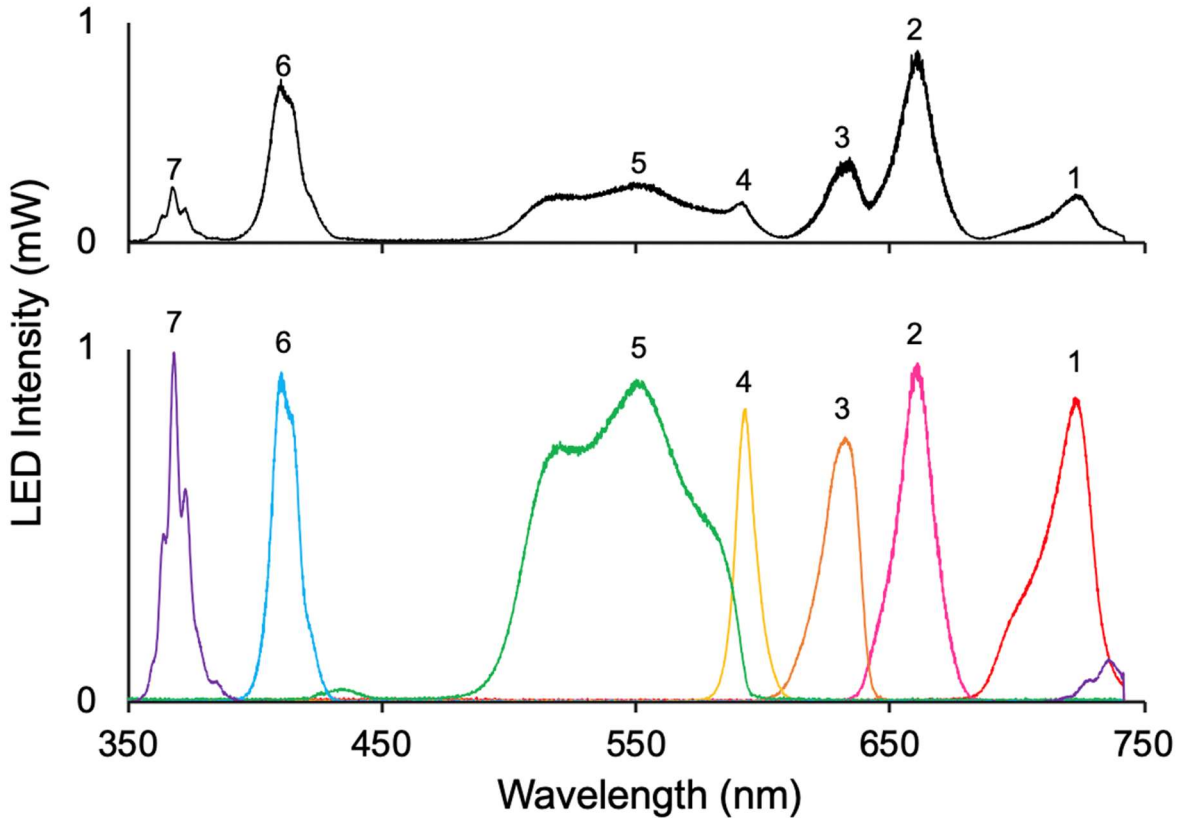

Fig. S6 | LED intensity. The LED bundle is composed of 7 distinct fibre-coupled LEDs, each of which is controlled by a separate channel in the software (Mightex). Spectral information for all LED channels was obtained by using an Optical Spectrum Analyser (Thorlabs). LED channel 1 (740 nm, Red), 2 (656 nm, Pink), 3 (625 nm, Orange), 4 (590 nm, Yellow), 5 (560 nm, Green), 6 (410 nm, Blue), 7 (365 nm, Purple). Some LED channels illuminate at a higher intensity than others. Top: All LED channels are simultaneously turned on and run at 10 mA. Bottom: Each LED channel was separately turned on (illuminating at their maximum intensity) and the resulting traces of all seven LEDs superimposed. Some LED channels illuminate over a broader band of wavelengths, and at a higher intensity, than others.

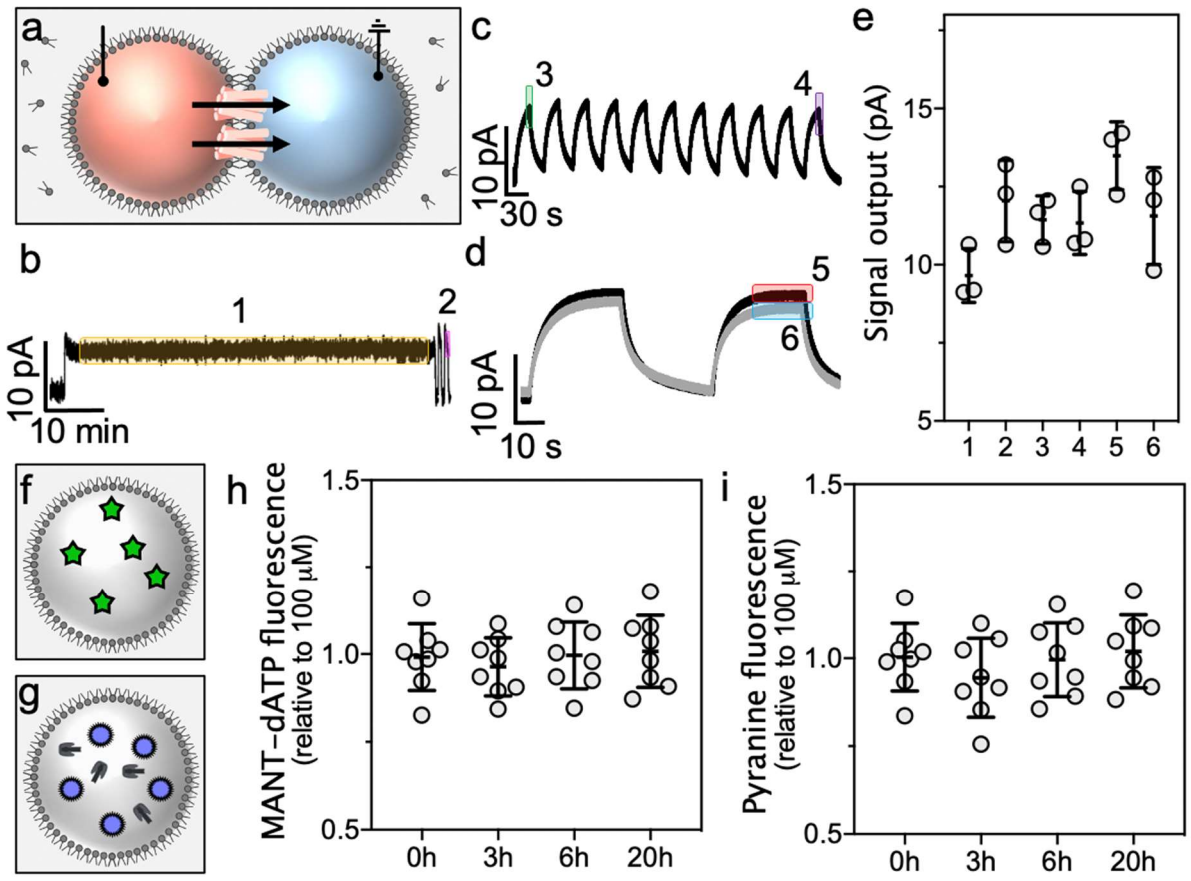

Fig. S7 | Resistance of CM-aR3, MANT-dATP and pyranine to photobleaching. a, Schematic of the CM-aR3 photobleaching experiment. A DIB containing CM-aR3 is formed with Ag/AgCl electrodes inserted into the droplets. The recording electrode is in the sensory (protein-containing) droplet (pink) and the ground electrode in the axon droplet (protein-free, blue). **b-d,** Sample traces of signals recorded across the sensory DIB. b: Prolonged illumination (1 h, YG light) then two short pulses (30 s, 0.01ὸ Hz) after 1 minute in the dark. c: Frequent rapid pulses (11 pulses of 30 s, 0.01ὸ Hz, YG light). d: Illumination with two short pulses (YG light, 30s, 0.01ὸ Hz) before (black) and after (grey) prolonged illumination (20 h, YG light). Steady-state signals are boxed and numbered 1-6. **e,** Average steady-state signal outputs (shown in the boxes in 'b-d') are comparable in magnitude, indicating no loss of the retinal chromophore by 'photobleaching' of CM-aR3 under our experimental conditions. n = 3 DIBs. **f,g,** Schematics of droplet containing f: pyranine (green stars) and g: MANT-dATP (purple spheres) and αHL (black) for photobleaching experiments. **h-i,** Fluorescence of h: pyranine dye and i: MANT-dATP dye at different time points after continuous illumination with YG light. n = 8 droplets.

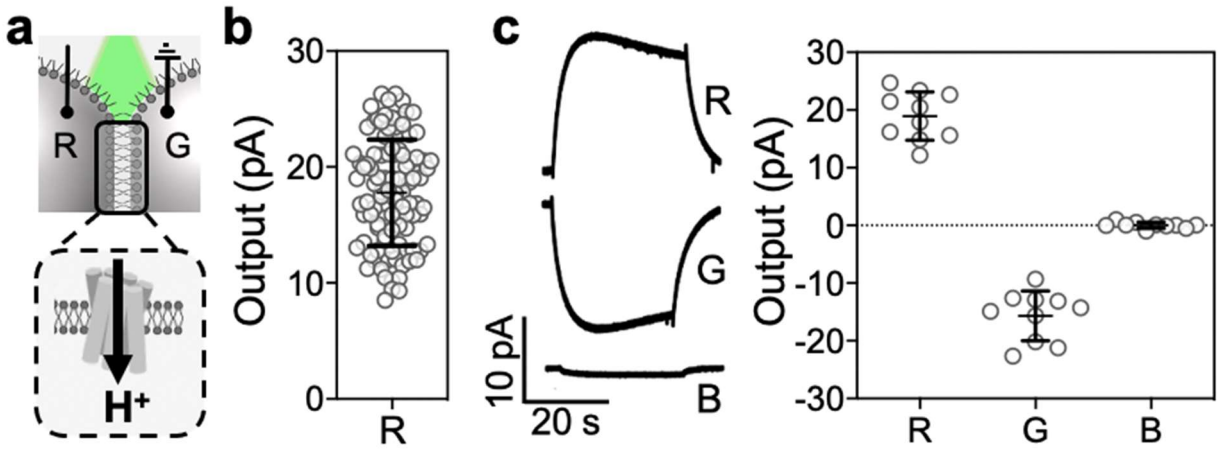

Fig. S8 | CM-aR3 inserts N-terminus first into the bilayer. a, Schematic of a sensory bilayer. The droplets contain a recording (R) or ground (G) electrode (Ag/AgCl) for electrical recording. Upon illumination with YG light (green), CM-aR3 pumps hydrogen ions (H^+) across the bilayer generating a signal. **b,** Signal output generated when a CM-aR3-containing sensory bilayer is illuminated (n = 100 independent bilayers). Sensory droplets contain CM-aR3 and the recording electrode. All output signals are positive (i.e., H^+ pumping is out of the sensory droplet, see Materials and Methods). The CM-aR3 was from 13 different batches (prepared between 2016 - 2020 but following the same protocol); all final sensory droplets contained 100 mM MES, 100 mM NaCl, 0.001% DDM and 0.15 – 0.25 mg mL^{-1} CM-aR3. **c,** ***Left:*** Typical signal trace recorded when the CM-aR3 is in the droplet containing the recording electrode (R) or the ground electrode (G) or in both droplets (B). *Right:* Steady-state signal output recorded across the CM-aR3-containing sensory bilayer upon illumination (mean ±SD, n = 10 independent DIBs). In this case, the CM-aR3 was from the same protein expression batch.

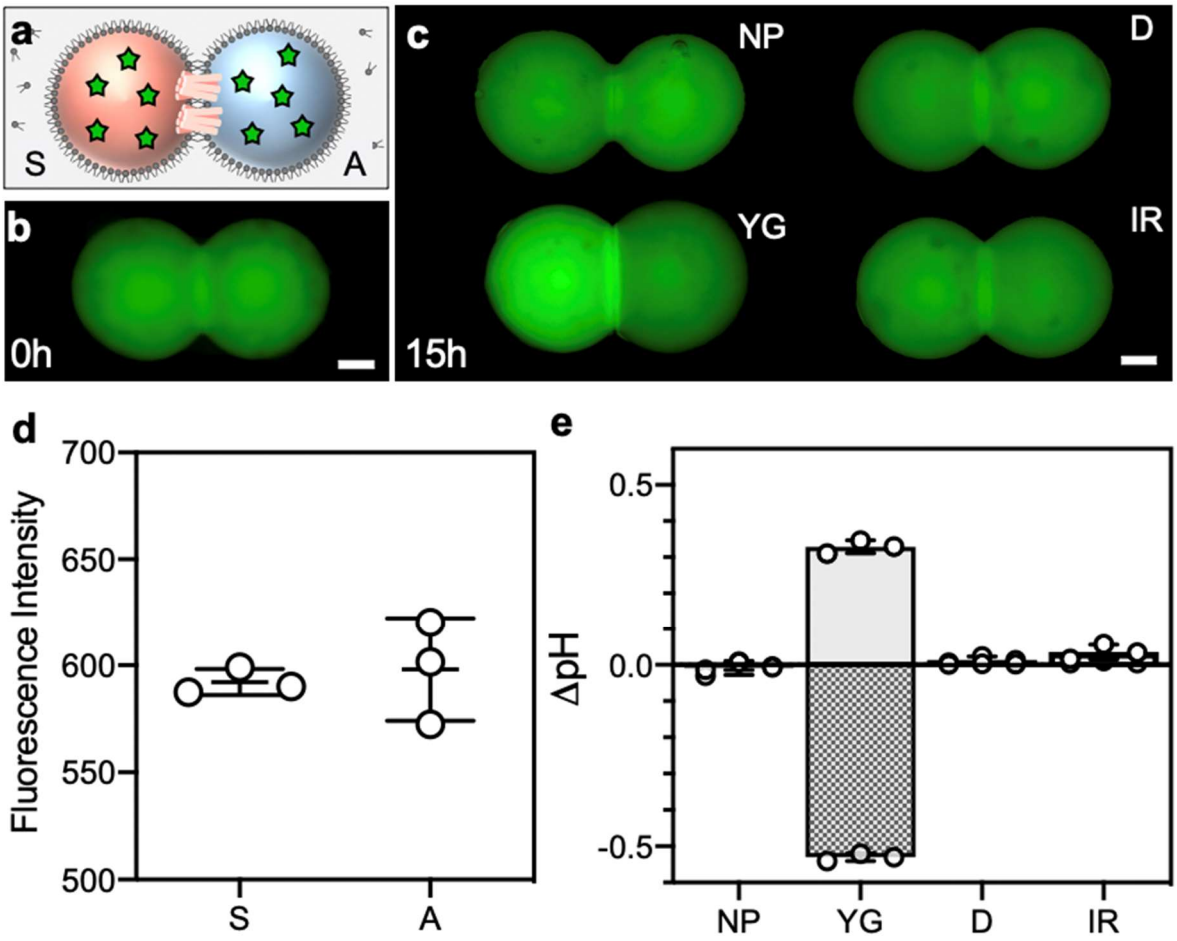

Fig. S9 | YG light mediates hydrogen ion pumping. a, Schematic of a sensory bilayer with both droplets containing the pH-sensitive dye pyranine (green stars). The sensory droplet (S, pink) contains CM-aR3. No electrodes are used here. **b,** Typical epifluorescence image (minus background) of the sensory bilayer at the start (0 h) of an experiment; both droplets are at pH 6.5. Scale bar = 200 μm. **c,** Typical epifluorescence images (minus background) of the sensory bilayer after: Illumination with YG light (15 h) either in the presence (YG) or absence (no protein, NP) of CM-aR3 in the sensory bilayer. Illumination with IR light (15 h); or no illumination (dark, D) (15 h). Scale bar = 200 μm. **d,** Initial fluorescence intensity (minus background fluorescence) of the sensory (S) and axon (A) droplets (mean ± SD of 3 images of n = 3 independent droplet pairs). **e,** Change in pH (mean ± SD of 3 images of n = 3 independent droplet pairs) of the sensory (S, grey) and axon (A, striped grey) droplets after illumination with YG light (15 h) either in the presence (YG) or absence (no protein, NP) of CM-aR3 in the sensory bilayer; illumination with IR light (15 h); or no illumination (dark, D) (15 h).

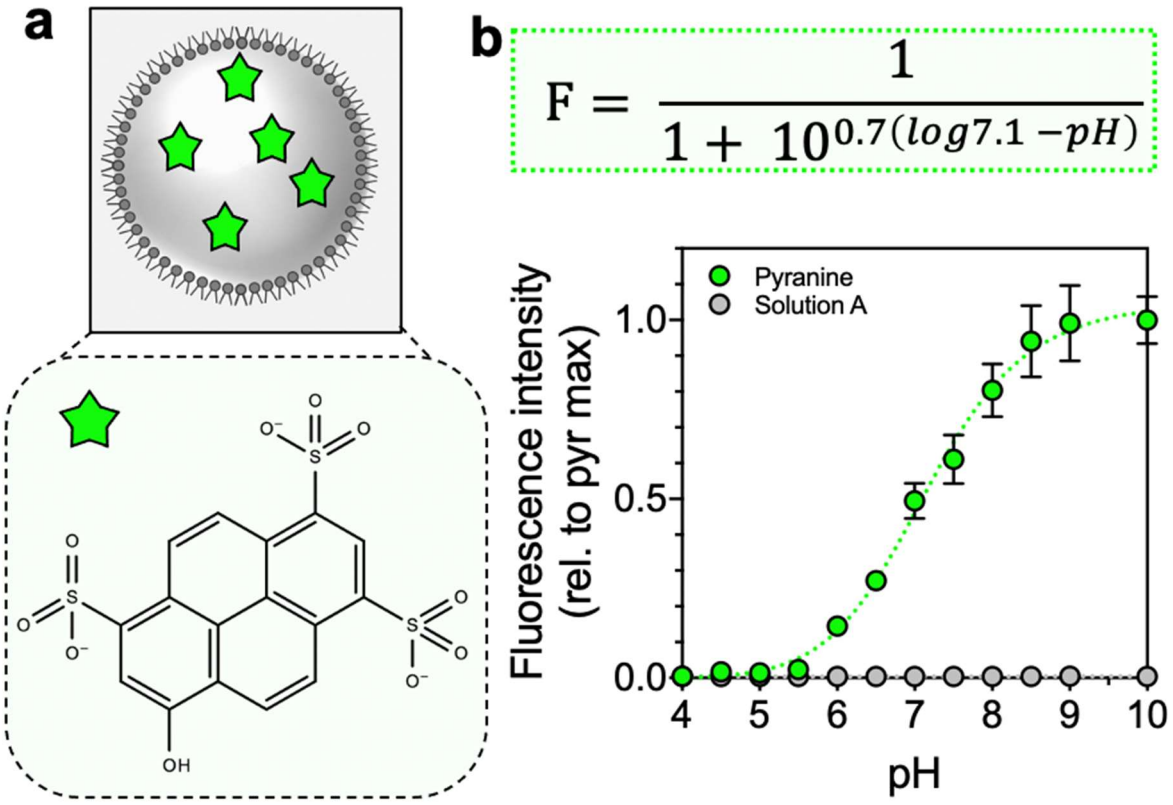

Fig. S10 | Calibration curve of the pH-sensitive dye, pyranine. a, Schematic of a pyranine (green star) containing droplet. Zoom: structure of pyranine, drawn in PubChem Sketcher[11]. **b,** The fluorescence intensity (mean ± SD, relative to pyranine droplet maximum i.e., fluorescence intensity recorded in a droplet with pH 10) of a droplet (200 nL, containing pyranine dye = green, or in the absence of dye = grey) was plotted against the internal pH (n = 8 independent droplets, see Materials and Methods). The sigmoidal curve fit (dotted line) gives the equation shown and generates a pK_a value of 7.3 (literature value ~7.2 - 7.3[3]). Integer values for the sigmoidal fit equation are to 1 decimal place. A relative fluorescence of 1 corresponds to a fluorescent intensity of 2156.

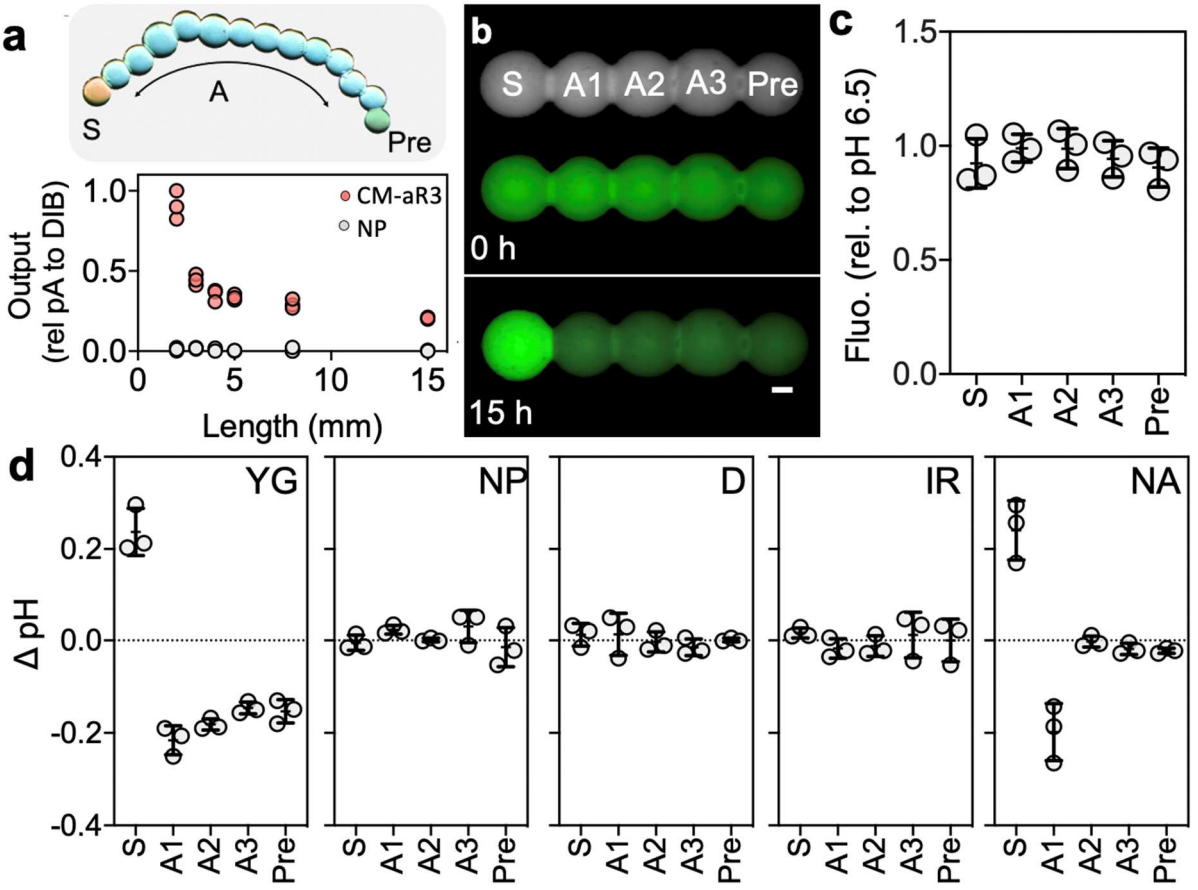

Fig. S11 | Transmission along a droplet synthetic axon. a, *Top:* Photograph of a droplet-based synthetic neuron (background removed, see Materials and Methods). The sensory droplet (200 nL, pink, S) contains 100 mM MES, 100 mM NaCl, pH 6.5 and 0.15 - 0.25 mg CM-aR3 mL^{-1}. The droplet (200 nL) which forms a DIB with this sensory droplet (A1) contains 100 mM NaCl, pH 6.5. All other droplets (200 nL) contain 100 mM NaCl, pH 6.5 and 50 nM αHL. The recording electrode is in the CM-aR3 sensory droplet (S) and the ground electrode in the terminal presynaptic droplet (Pre). *Bottom:* Dependence of the signal output recorded across a droplet neuron on the number of droplets, relative to that of a droplet pair. **b,** Epifluorescence microscopy images (minus background) of a 5-droplet synthetic neuron before (0 h) and after illumination (YG light, 15 h). Scale bar = 200 μm. The droplet neuron is composed of a sensory droplet (S), 3 axon droplets (A1, A2, A3) and a presynaptic droplet (Pre). All droplets contain the pH-sensitive dye pyranine; fluorescence intensity increases with pH (Fig. S11). **c,** Droplet fluorescence before illumination (minus background fluorescence) relative to that of a pH 6.5 pyranine droplet. **d,** Change in droplet pH (n = 3 synthetic neurons) after illumination with YG light (15 h). Controls were performed in the absence (NP) of CM-aR3 and absence of αHL (NA) or when the neuron was illuminated with IR light (IR) or kept in the dark (D).

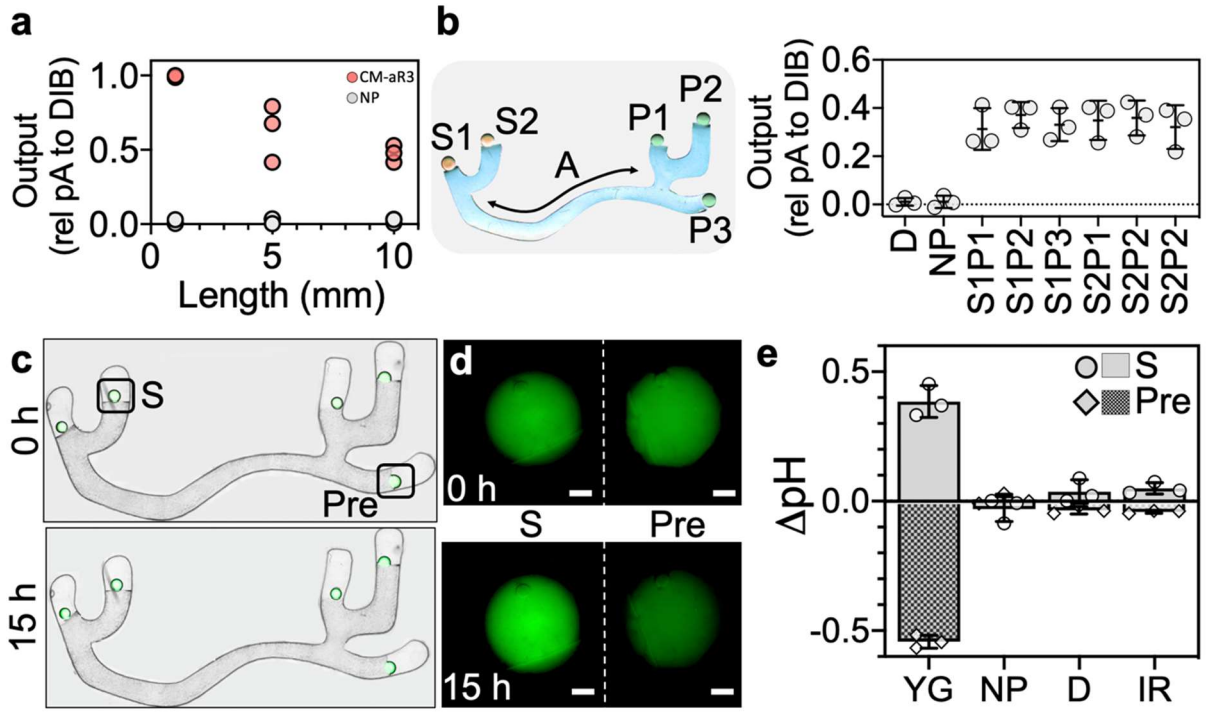

Fig. S12 | Transmission along a hydrogel synthetic axon. a, Signal output recorded across a hydrogel neuron as the axon increases in length. At either end of the axon are the sensory droplet (200 nL, 100 mM MES, 100 mM NaCl, pH 6.5, containing 0.15 - 0.25 mg CM-aR3 mL^{-1}) and the presynaptic droplet (100 mM NaCl, pH 6.5, containing 50 nM αHL). Datapoints are plotted relative to the mean output of a droplet pair. A control was performed in the absence of CM-aR3 (NP, grey) and no output was generated. **b,** Photograph of a hydrogel-based synthetic neuron (background removed, see Materials and Methods). In this case, there are two sensory droplets (S1, S2) and three presynaptic droplets (P1, P2, P3). The signals are recorded between different droplets in the branched hydrogel neuron. The signal path is indicated ([n,m]: sensory droplet number followed by presynaptic droplet number). The sensory droplet contains the recording electrode and the presynaptic droplet the ground electrode. Controls in the absence of light (D) and absence of CM-aR3 were also performed for the S1P1 pathway. **c,** Composite image of the brightfield and fluorescence images of a hydrogel neuron before (0 h) and after (15 h) illumination. Only the terminal droplets contain the pyranine dye. Images are stitched together (see Materials and Methods). **d,** Epifluorescence microscopy images (minus background) of the sensory (S) and presynaptic (Pre) droplets before and after illumination (YG light, 15 h). Scale bar = 200 μm. **e,** Change in droplet pH (n = 3 synthetic neurons) when the neuron is illuminated with YG light in the presence (YG) or absence (NP) of CM-aR3 or illuminated with IR light (IR) or kept in the dark (D).

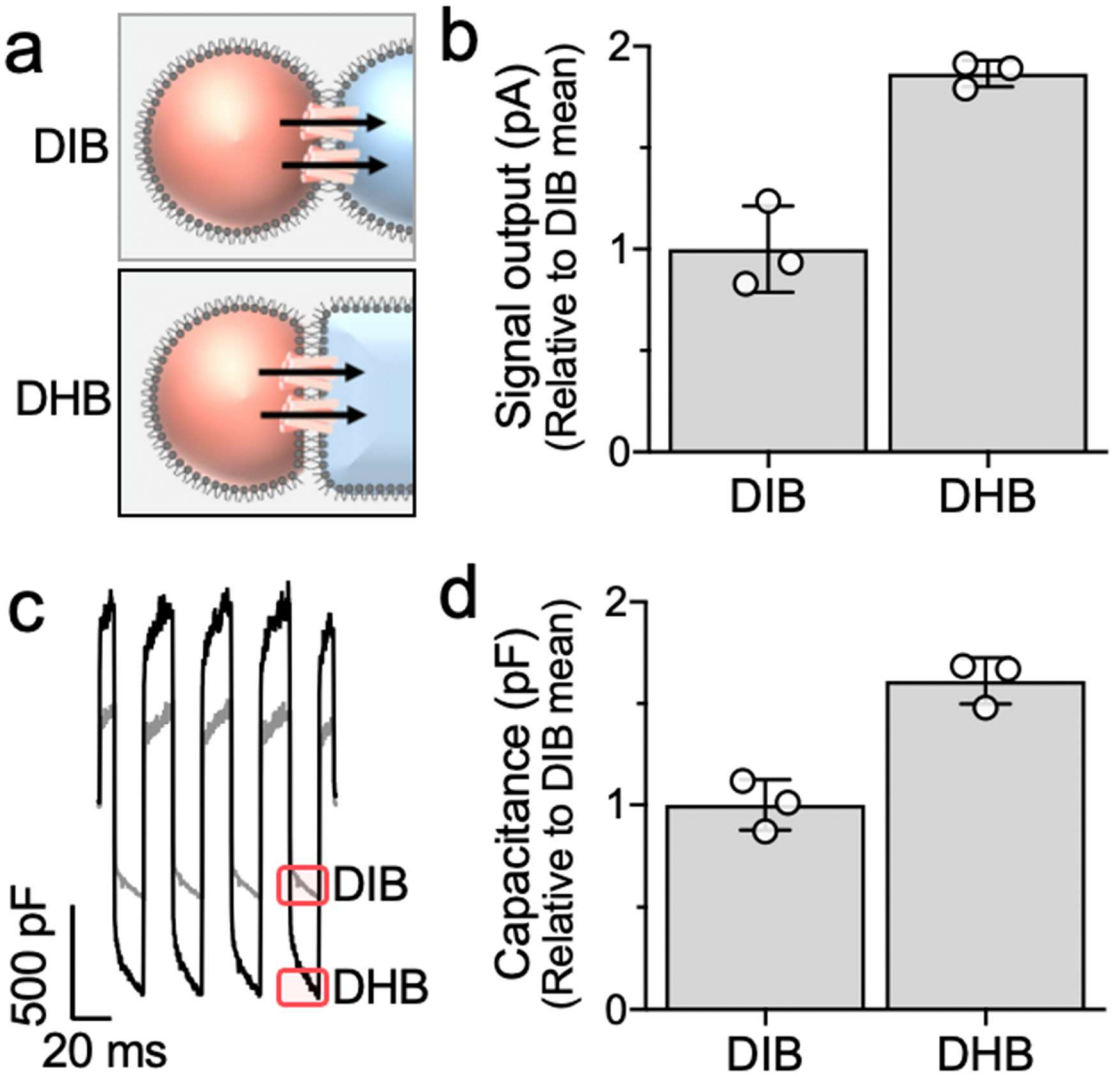

Fig. S13 | DIB and DHB comparison. a, Schematic of a droplet interface bilayer (DIB) and droplet hydrogel bilayer (DHB) containing CM-aR3. Ag/AgCl electrodes are inserted into the droplets with the recording electrode in the CM-aR3-containing sensory droplet (pink) and the ground electrode in the axon droplet (blue, DIB) or hydrogel (blue, DHB). **b,** Signal output recorded across CM-aR3-containing DIBs and DHBs when illuminated with YG light. The mean signal generated by CM-aR3-containing DIBs (n = 3 independent bilayers) is normalized to a value of 1 and the output from a DHB is plotted relative to this. **c,** Sample signal trace of a capacitance recording (in the dark) across a CM-aR3-containing DIB (grey) and a CM-aR3-containing DHB (black) (n = 1 bilayer). **d,** Capacitance values for CM-aR3-containing DIBs and DHBs. The mean capacitance of the CM-aR3-containing DIBs is normalized to a value of 1 (n = 3 independent bilayers) and the capacitance values of DHB are plotted relative to this.

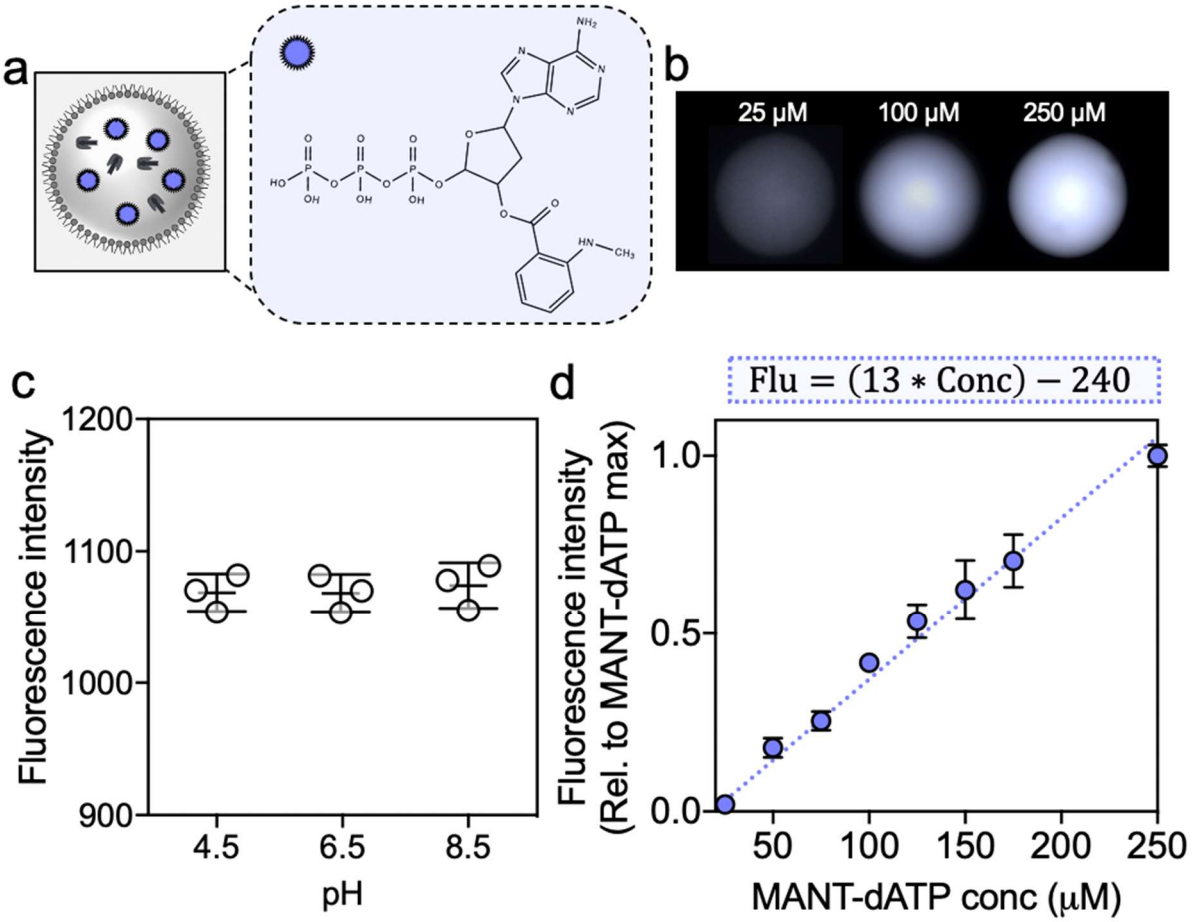

Fig. S14 | MANT-dATP fluorescence calibration curve. a, Schematic of a presynaptic droplet containing 100 mM NaCl, 100 mM MES, αHL (50 nM), MANT-dATP (purple stars, 100 μM), pH 6.5. Zoom: MANT-dATP drawn using PubChem Sketcher[11]. **b,** Epifluorescence images of droplets containing MANT-dATP at 25 μM, 100 μM, and 250 μM. **c,** Fluorescence of MANT-dATP at different droplet pH values (n = 3 independent droplets, see Materials and Methods). Droplet pH has no effect on MANT-dATP fluorescence intensity. **d,** Calibration curve of fluorescence intensity against MANT-dATP concentration. A straight-line fit (dotted line, integer values to 2 significant figures, mean $\pm$ SD, n = 8 independent droplets, see Materials and Methods) with equation F = (13*C) - 240 describing the relationship. Concentrations below 18 µM (2 significant figures) were not detectable with our fluorescence microscopy set-up.

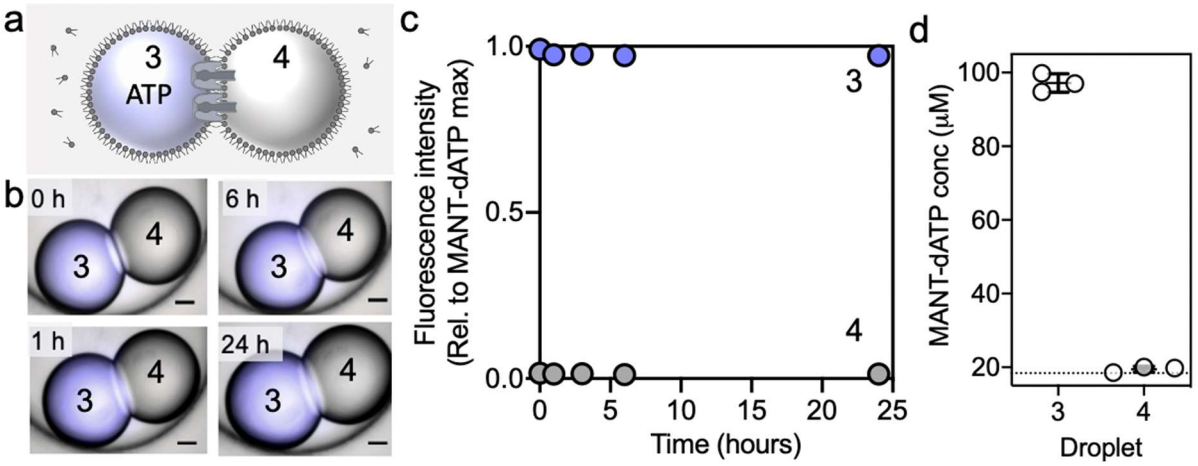

Fig. S15 | Spontaneous movement of MANT-dATP through αHL in the absence of an electrochemical potential gradient. a, Schematic of synaptic bilayer formed between the presynaptic (3, purple, 50 nM αHL, 100 μM MANT-dATP, 100 mM MES, 100 mM NaCl, pH 6.5) and postsynaptic (4, grey, 100 mM MES, 100 mM NaCl, pH 6.5) droplets. **b,** Brightfield and fluorescence microscopy image overlay of a (tetherless) synthetic synapse over time (0h, 1h, 6h and 24 h) in the absence of an applied potential. The presynaptic (3) and postsynaptic (4) droplets are labelled. **c,** Fluorescence intensity over time (mean $\pm$ SD, n = 3 independent DIBs, see Materials and Methods) of the presynaptic (3, purple) and postsynaptic (4, grey) droplets. **d,** MANT-dATP concentration in the presynaptic (3) and postsynaptic (4) droplets after 24 h (in the absence of an applied potential, n = 3 independent DIBs, see Materials and Methods). The detection limit (dotted line) is at 18.4 μM MANT-dATP.

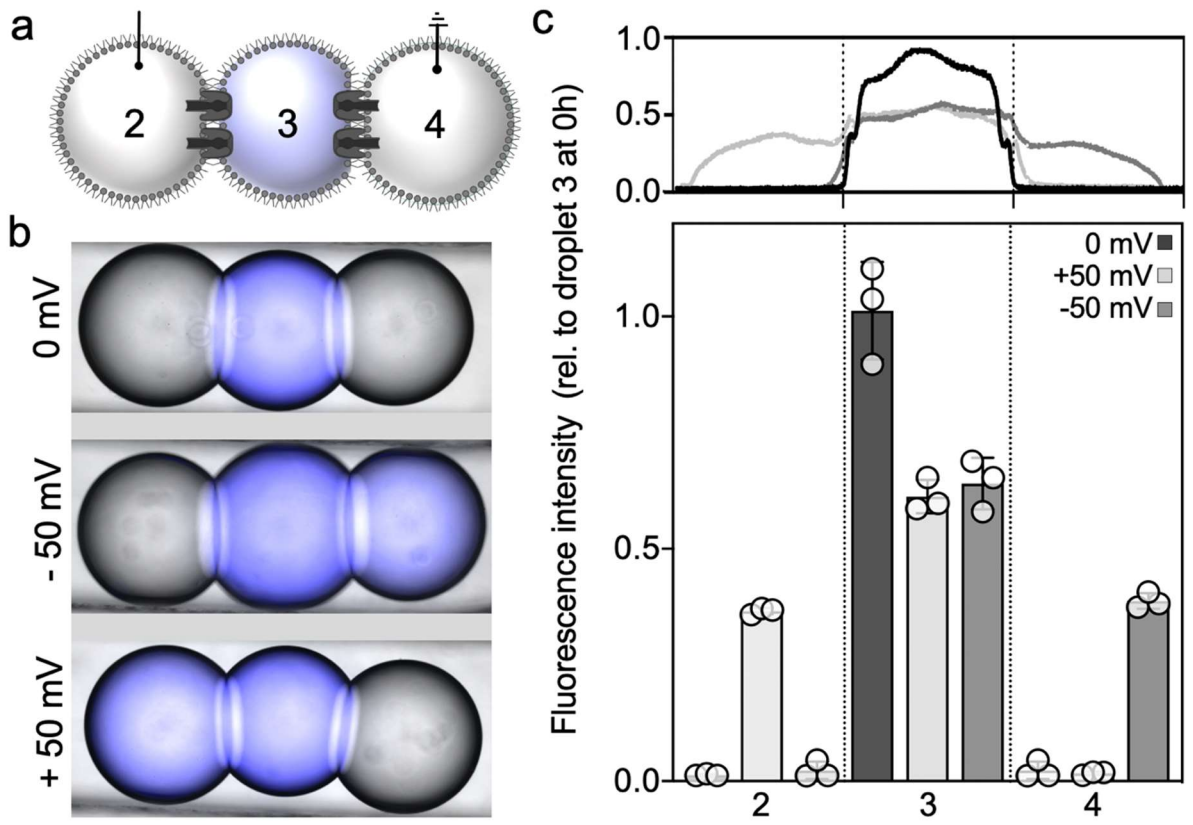

Fig. S16 | An applied potential moves MANT-dATP across the synaptic bilayer. a, Schematic of a 3-droplet chain formed from an axon droplet (2), presynaptic droplet (3) and postsynaptic droplet (4). The presynaptic droplet (3) contains 50 nM αHL, 100 μM MANT-dATP, 100 mM NaCl, pH 6.5. Ag/AgCl electrodes (tethers) are inserted into the terminal droplets (2, 4); the ground electrode is in the postsynaptic droplet (4). **b,** Composite image (bright-field and epifluorescence images overlayed) of the 3-droplet chain after 1 h with an applied potential of 0 mV, -50 mV or +50 mV. Overlapping images are stitched together (see Materials and Methods). **c,** *Top:* Fluorescence intensity of the 3-droplet chains shown in 'b' after 1 h with an applied potential of 0 mV (black), -50 mV (light grey) or +50 mV (dark grey). *Bottom:* Fluorescence intensity of MANT-dATP (mean ± SD, n = 3 independent droplet chains) in the axon (2), presynaptic (3) and postsynaptic (4) droplets after 1 h with an applied potential of 0 mV (black), -50 mV (light grey) or +50 mV (dark grey). Each datapoint is the average of three images of the same droplet chain. A fluorescence intensity of 1.0 corresponds to a MANT-dATP concentration of 100 μM.

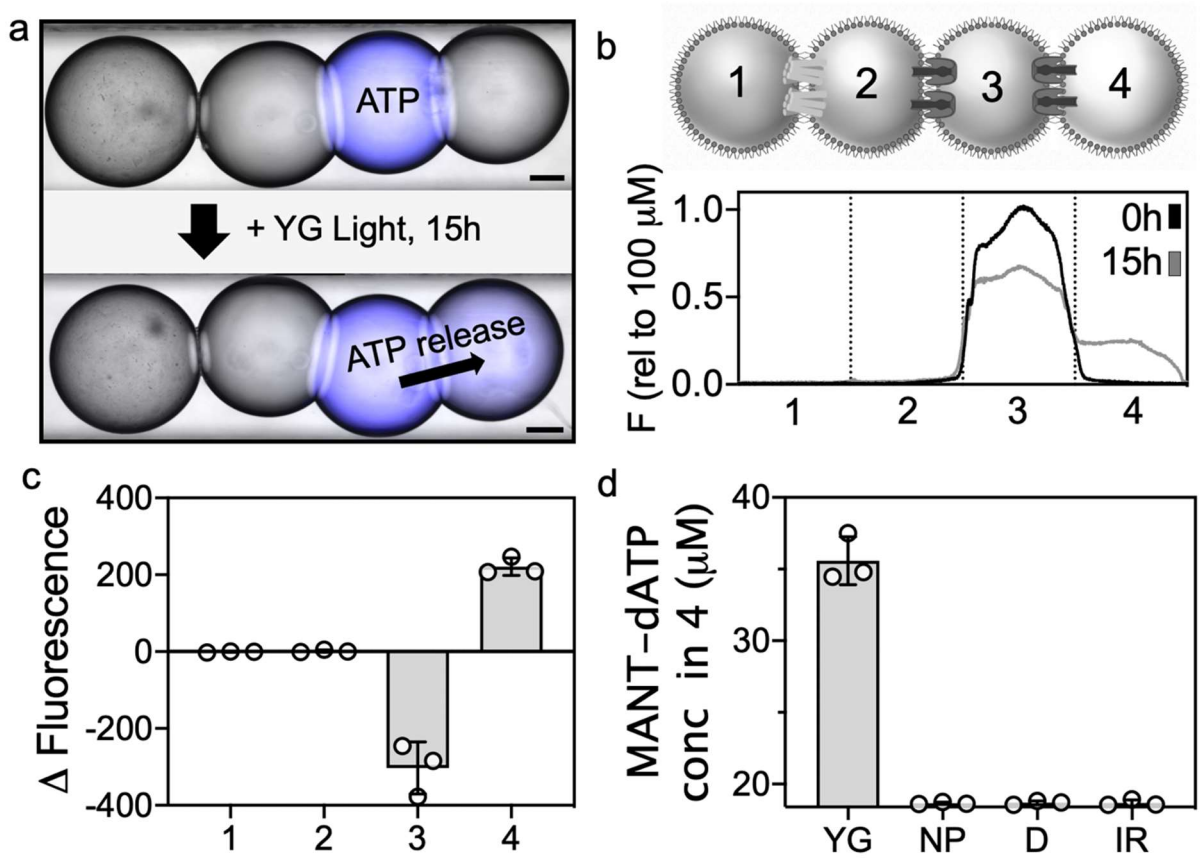

Fig. S17 | Neurotransmitter release from a synthetic 4-droplet neuron. a, Composite images (bright-field and epifluorescence images overlayed) of a 4-droplet synthetic neuron before and after illumination (15 h, YG light). MANT-dATP is transported across the synaptic bilayer. Overlapping images are stitched together (see Materials and Methods). Scale bar = 200 μm. **b,** *Top:* Schematic of a droplet synthetic neuron composed of a sensory (1), axon (2), presynaptic (3) and postsynaptic (4) droplet. Sensory droplets contain CM-aR3 and presynaptic droplets contain MANT-dATP and αHL. *Bottom:* Fluorescence intensity of a 4-droplet synthetic neuron shown in 'a' before (black, 0h) and after (grey, 15h) illumination. The neuron cross-section is plotted relative to the fluorescence intensity of a 100 μM MANT-dATP containing droplet. **c,** Change in fluorescence intensity of each droplet (as shown in 'a') after overnight illumination (mean ± SD, n = 3 synthetic neurons, each datapoint is the average of three images of the same synthetic neuron). **d,** MANT-dATP transferred to the postsynaptic droplet (4) when the synthetic neuron is illuminated with YG light in the presence (YG) or absence (NP) of CM-aR3 or left in the dark (D) or illuminated with IR light (IR). The y-axis starts at the detection threshold = 18.4 μM.

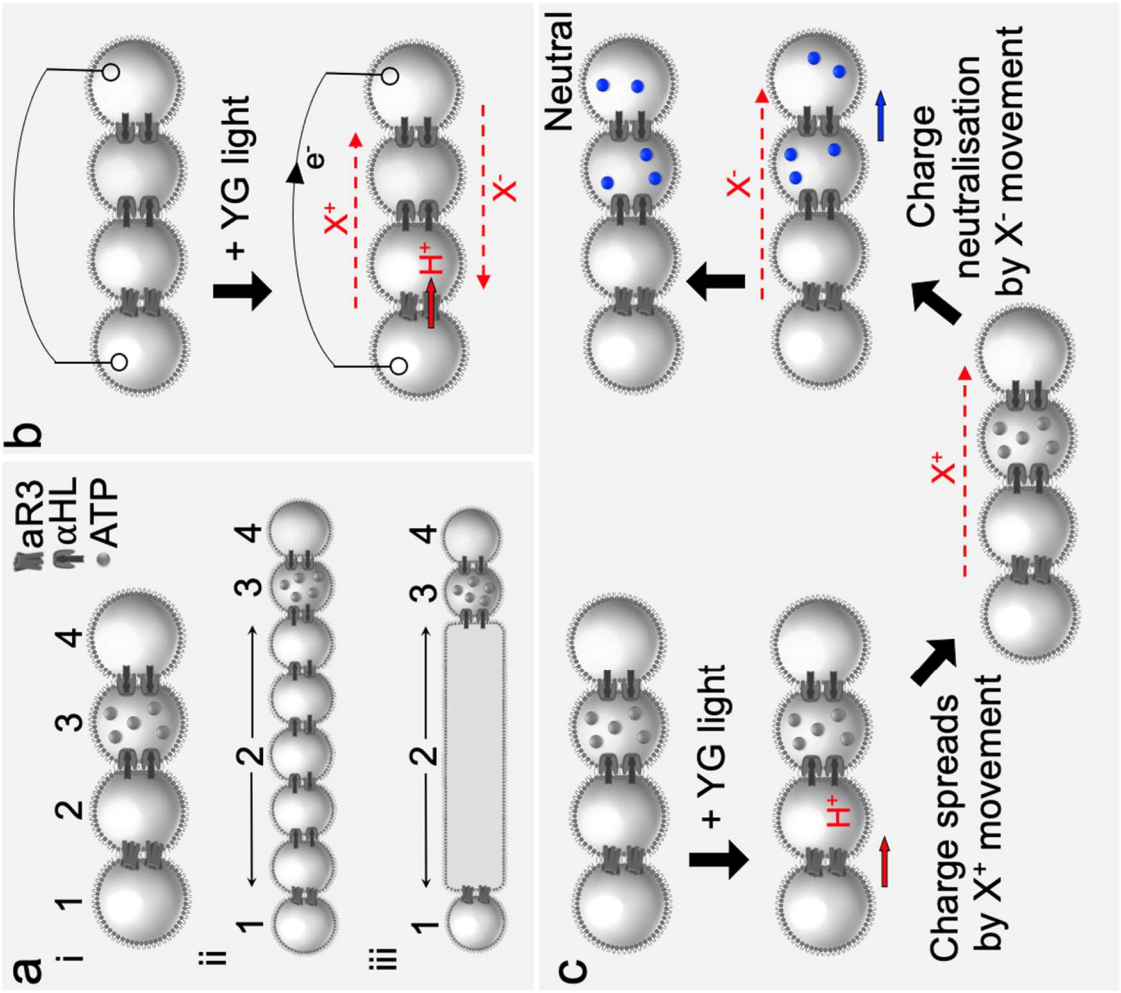

Fig. S18 | Ion and molecule movement in a synthetic neuron. Signal transmission in a synthetic neuron. **a,** i A four-droplet system is shown: sensory (1), axon (2), presynaptic (3) and postsynaptic (4) droplets. Presynaptic droplet contained the ATP neurotransmitter. First, the sensory and synaptic bilayers (between droplets 1-2 and 3-4 respectively) were built. Then, the pathway was completed by joining droplets 2-3. After bilayer formation, protein inserts into the new interface. The same principle would apply in 'ii' an extended droplet system in which additional droplets containing αHL form the axon or 'iii' in the case where the axon is replaced by a conductive hydrogel axon. **b,** Transmission in the presence of an external circuit. In this case, compensating charge can be provided at the Ag/AgCl electrodes. Upon irradiation, H^+ leaves droplet 1 and moves into droplet 2. At the electrode in droplet 1: $Ag \rightarrow Ag^+$ and Cl^- is picked up from solution, and the (electron) e^- from the oxidation of Ag moves to droplet 4 as a measurable current in the external circuit. At the electrode in droplet 4: Cl^- moves into solution to neutralise the positive charge arising from H^+ pumping. The e^- from droplet 1 converts $Ag^+ \rightarrow Ag$ maintaining charge neutrality at the electrode in droplet 4. X^+ = cation, X^- = anion. **c,** Transmission in the absence of an external circuit. Upon irradiation, hydrogen ions (H^+) are pumped electrogenically from droplet 1 into droplet 2; this DIB contains no αHL pores. The charge in droplet 2 then spreads throughout the neuron by using the pores at the interfaces 2/3 and 3/4. The charge is carried by H^+, and by other ions (X^+). The positive charge in droplets 2-4 is then slowly neutralised by the movement of the weakly bilayer-permeant Cl^- across interface 1/2 (in the absence of pores). Again, the charge can be carried by other ions (X^-), which would include the movement of negatively charged 'transmitter' molecules from droplet 3 to droplet 4, including MANT-dATP^{4-} or ATP^{4-}. The diffusion of some MANT-dATP^{4-} or dATP^{4-} from drop let 3 to droplet 2 will eventually occur.

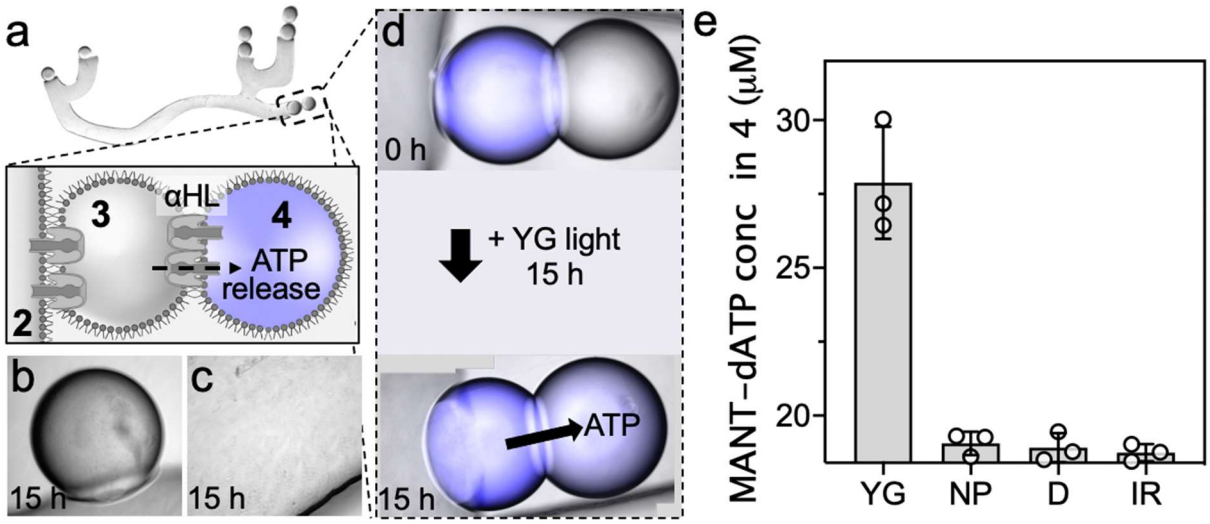

Fig. S19 | Neurotransmitter release from a synthetic hydrogel neuron. a, Photograph (background removed) of a synthetic neuron. Zoom: synaptic terminal of a synthetic neuron: axon (2), presynaptic droplet (3), postsynaptic droplet (4). MANT-dATP is released by transport through αHL pores in the synaptic bilayer. **b-c,** Bright-field and fluorescence microscopy overlays of b: the sensory droplet and c: the hydrogel axon (2) after illumination (15 h, YG light). **d,** Bright-field and fluorescence microscopy overlays of the synaptic terminal before and after illumination (15 h, YG light). Overlapping images are stitched together (see Materials and Methods). **e,** MANT-dATP transferred to the postsynaptic droplet (4) after the synthetic neuron was illuminated (for 15 h) with YG light in the presence (YG) or absence (NP) of CM-aR3, or left in the dark (D), or illuminated with IR light (IR). The y-axis starts at the detection threshold = 18.4 μM. n = 3 independent synthetic neurons.

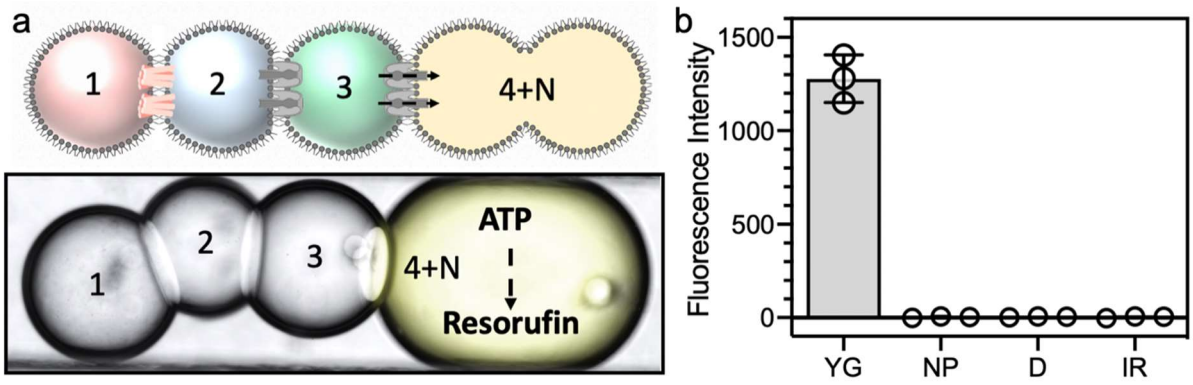

Fig. S20 | Downstream signalling in a synthetic 4-droplet neuron. a: Top: Schematic of a droplet synthetic neuron composed of sensory (1, pink), axon (2, blue) and presynaptic (3, green) droplets, and fused postsynaptic and neighbouring (4+N yellow) droplets. Sensory droplets contain CM-aR3, presynaptic droplets contain ATP and αHL and neighbouring droplets contain a reaction mixture (all the precursors and enzymes of a biochemical ATP-dependent reaction). Bottom: Bright-field and epifluorescence microscopy overlay of the droplet neuron after the downstream reaction has occurred. The neuron is illuminated for 15 h with YG light and then following fusion (4 + N) left for 0.5 h. Overlapping images are stitched together (see Materials and Methods). **b,** Change in fluorescence intensity of the fused postsynaptic and neighbouring droplets (4+N, yellow) after the synthetic neuron was illuminated with YG light in the presence (YG) or absence (NP) of CM-aR3 or left in the dark (D) or illuminated with IR light (IR). n = 3 independent synthetic neurons.

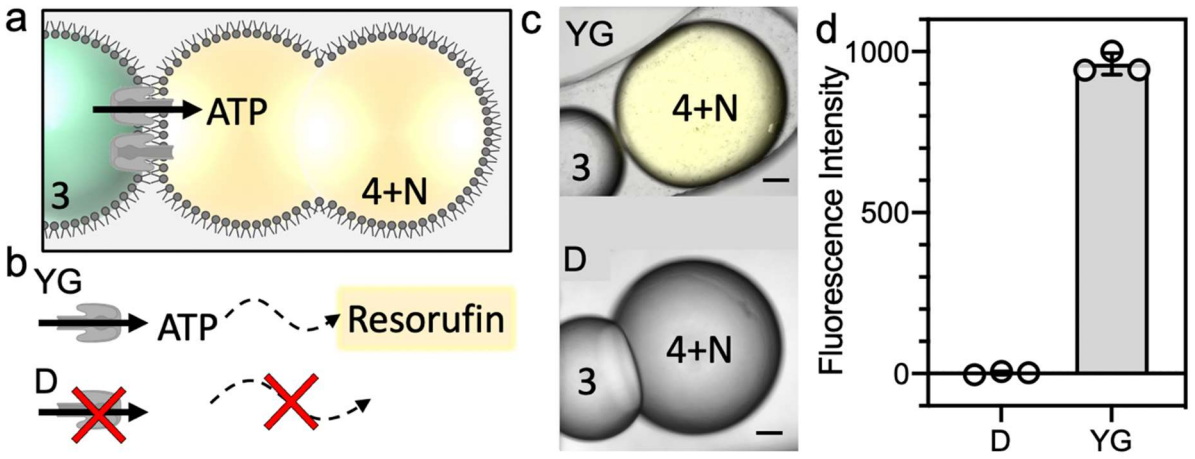

Fig. S21 | Downstream signalling in a synthetic hydrogel neuron. a, Schematic of the synaptic terminus of a 25 mm-long hydrogel synthetic neuron. The presynaptic droplet (3, green) contains the ATP neurotransmitter and the pore-forming protein αHL. Illumination of the synthetic neuron results in ATP transport through the αHL pores. Fusion (4+N) of the postsynaptic droplet (4), which contains released ATP, and the neighbouring droplet (N), which contains the ATP reaction components, enables ATP-dependent downstream reactions. **b,** Top: Under illumination (YG light) ATP is moved into the postsynaptic droplet (4). After fusion with the neighbouring droplet (N), the ATP-dependent downstream reactions occur and produce fluorescent resorufin. Bottom: If no ATP is released (when the synthetic neuron is in the dark (D)), no fluorescent product is produced. **c,** Composite images of the brightfield and fluorescence channels. Top: When the synthetic neuron is illuminated (YG light, 15 h), ATP is released and resorufin is produced. Bottom: In the dark (D, 15 h), no ATP is released and no resorufin is produced. Scale bar 200 μm. Overlapping images have been stitched together (see Materials and Methods). **d,** The change in fluorescence when the synthetic neuron is either illuminated with YG light or kept in the dark (dark, D) (n = 3 independent neurons).

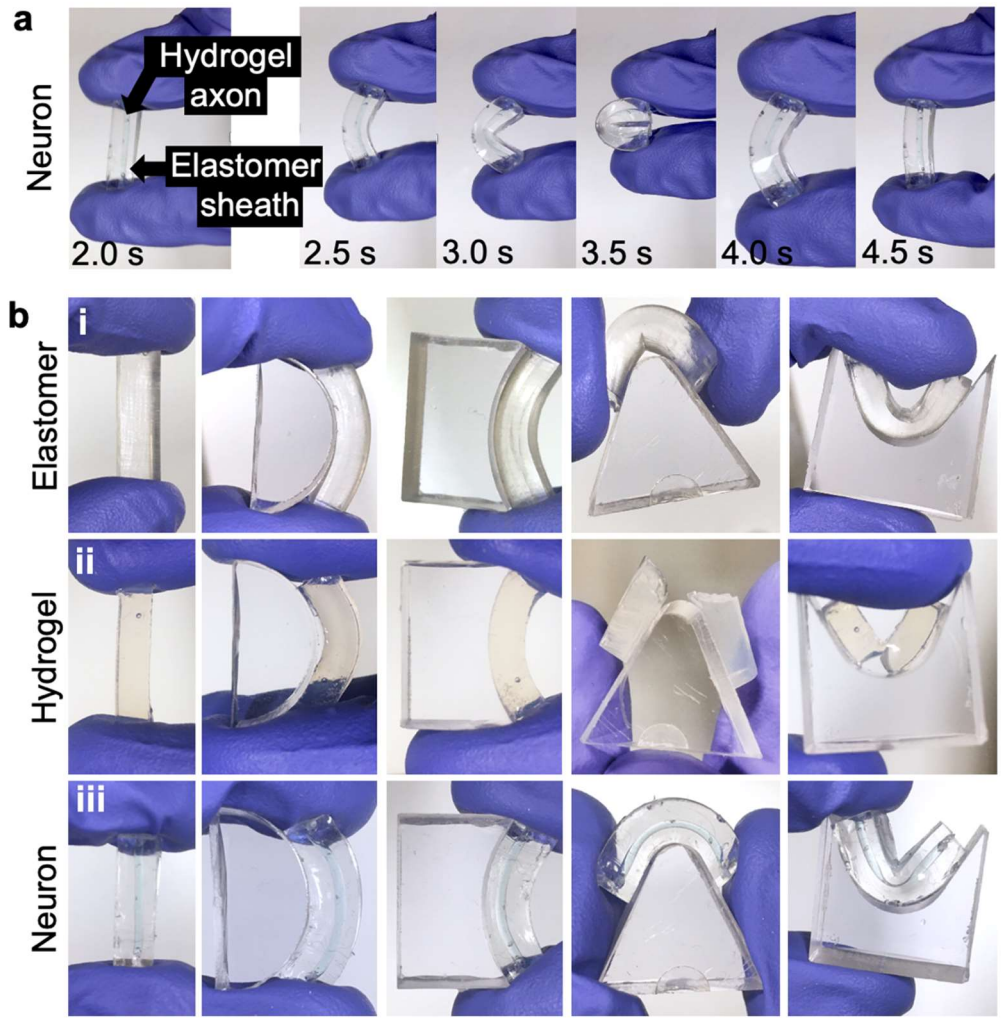

Fig. S22 | Biomaterial flexibility. a, A cuboidal synthetic neuron (length = 20 mm, width = 5 mm, height 5 mm) was bent between two fingers. The synthetic neuron is formed from an elastomeric sheath with a central hydrogel axon (2% agarose, cylindrical, length 20 mm, diameter 1 mm). The hydrogel axon contains blue food dye for visualisation. The synthetic neuron is flexible and can be repeatedly bent and allowed to return to its original shape. **b,** Cuboids of the biomaterials (length = 20 mm, width = 5 mm, height 5 mm) were placed over various curved plastic structures. (i) The elastomeric structure is flexible and can be positioned over all the structures without any permanent effect on its structural integrity. (ii) The hydrogel structure is less flexible. It can be positioned over structures with a shallow curvature, but fractures when forced over structures of higher curvature. (iii) The synthetic neuron (see 'a') is flexible and can be positioned over all the structures without any permanent effect on its structural integrity; The hydrogel axon within it remains intact. Images are typical of n = 3 cuboids.

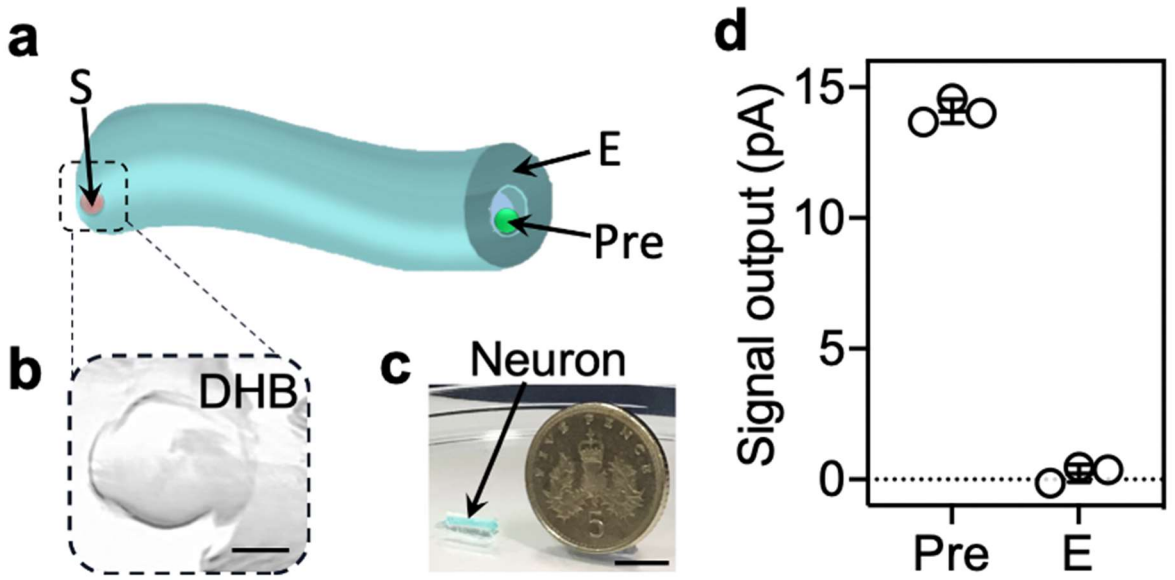

Fig. S23 | Insulated synthetic neuron. a, Schematic of an insulated synthetic neuron. The recording electrode is inserted into the CM-aR3 sensory droplet (S, pink). The ground electrode is inserted into the presynaptic droplet at the other end of the hydrogel axon (Pre, green) or into the elastomer sheath (E, teal). **b,** Zoom: brightfield image of the sensory droplet hydrogel bilayer (DHB, in oil). Scale bar: 200 μm. **c,** Photograph of the insulated synthetic neuron (in air). The central hydrogel neuron contains blue food dye for visualisation. Scale bar: 10 mm. **d,** Signal detected when the ground electrode is in the presynaptic droplet (Pre) or the elastomer sheath (E) (see 'a') and the synthetic neuron illuminated with YG light (mean ± SD, n = 3 independent neurons). A signal is transmitted along the synthetic axon to the presynaptic droplet (Pre) but not through the insulating sheath (E).

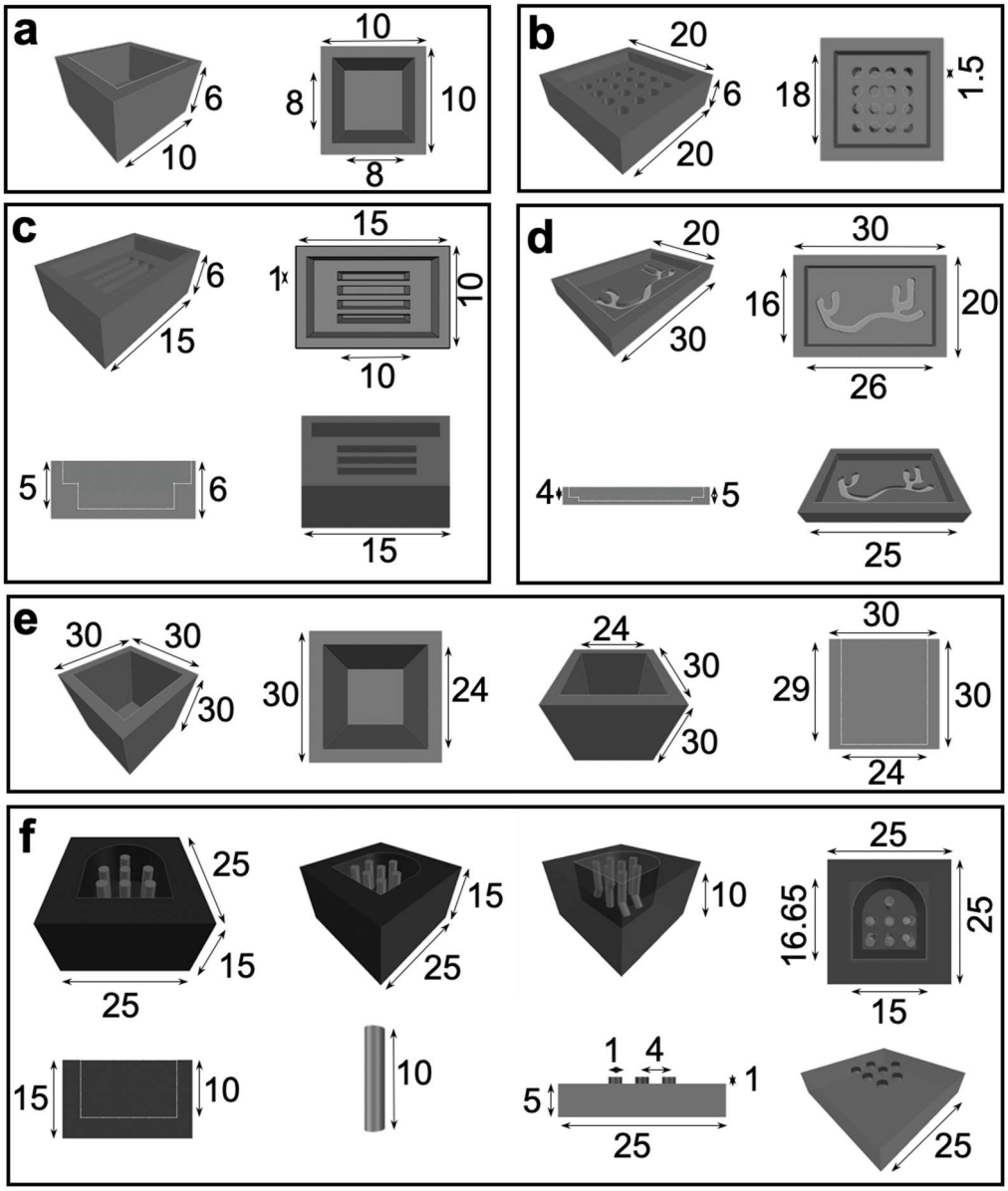

Fig. S24 | Synthetic neuron and nerve chamber design. AutoCAD software was used to design the bespoke (PMMA) chambers used: **a,** A droplet pair chamber for electrical recordings: outer dimensions of 10 x 10 x 6 mm and inner dimensions of 8 x 8 x 5 mm. **b,** A droplet array chamber for optical experiments: with outer dimensions of 20 x 20 x 6 mm and 16 wells with diameter 1.5 mm and height 5 mm. **c,** A neuron length electrophysiology chamber: outer dimensions of 15 x 10 x 6 mm and 4 trenches with dimensions of 10 x 1 x 5 mm. **d,** A branched neuron chamber for both electrophysiology and optical experiments: outer dimensions of 30 x 20 x 5 mm, inner dimensions of 26 x 16 x 3 mm and a hand-drawn neuron-shaped trench with a height of 1 mm and a diameter of ~ 1 mm. **e,** A synthetic nerve chamber for optical and electrical experiments with outer dimensions of 30 x 30 x 30 mm and inner dimensions of 24 x 24 x 29 mm. **f,** A synthetic nerve cast (first 6 images left to right) with outer dimensions of 25 x 25 x 15 mm and inner dimensions of 16.65 x 15 x 10 mm. The nerve cast contained seven cylindrical tubes with their centres spaced 4 mm apart (1 mm diameter and 10 mm height). The nerve cast had a lid (last 2 images, left to right) with outer dimensions of 25 x 25 x 5 mm and seven protruding tubes of height and diameter 1 mm. All dimensions are in millimetres and the chamber images are taken from the AutoCAD layout in perspective mode.

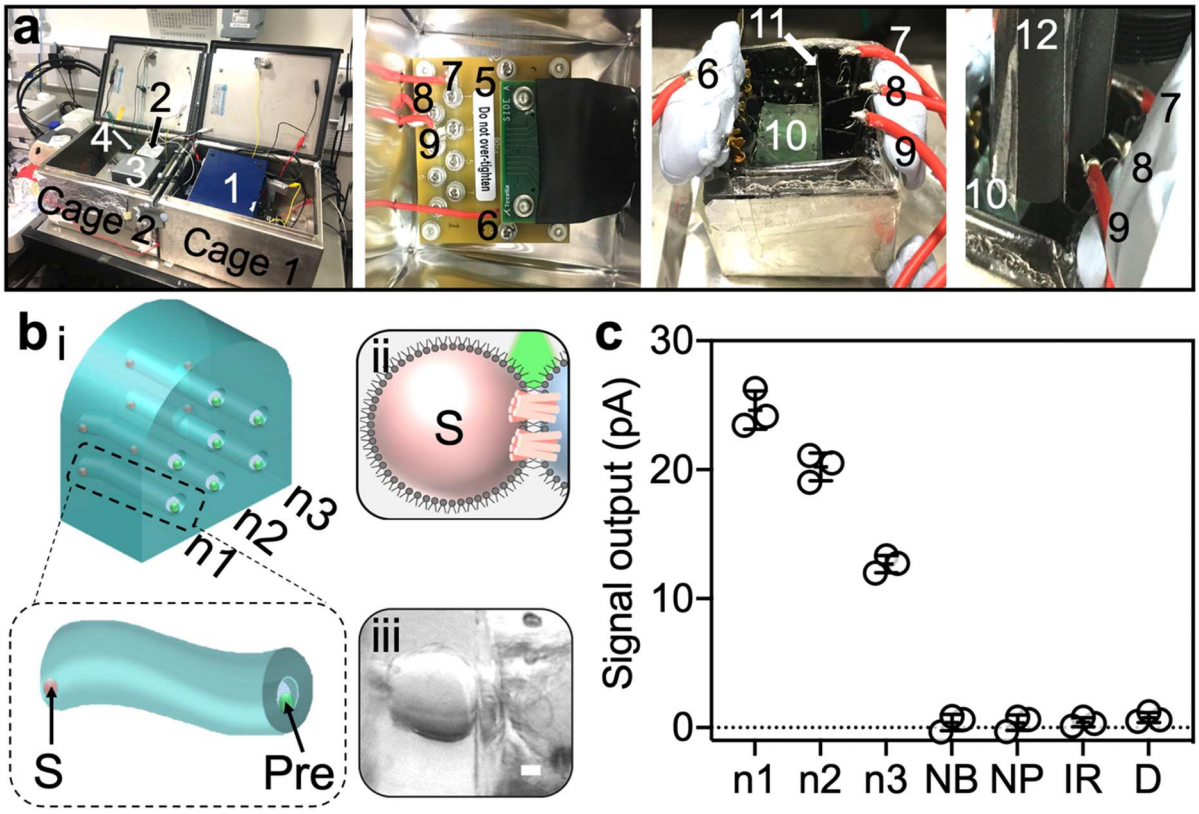

Fig. S25 | Synthetic nerve with a patterned stimulus. a, Photographs of the experimental set-up. *Left to Right:* The two Faraday cages. Cage 1: 1 – Multichannel amplifier. Cage 2: 2 – Aluminium box containing the terrapins, 3 – Metal cage, 4 – Location of the synthetic nerve and chamber. Photograph of the inside of the aluminium box (2): 5 – Terrapin, 6 – Ground electrode, 7 – Working electrode for axon n1, 8 – Working electrode for axon n2, 9 – Working electrode for axon n3. Wires (orange) are soldered to Ag/AgCl electrodes. Photograph of nerve chamber (coated in aluminium foil for light insulation): 6 – Ground electrode, 7 – Working electrode for axon n1, 8 – Working electrode for axon n2, 9 – Working electrode for axon n3, 10 – Synthetic nerve, 11 – Light sheets (waterproof black cardboard). LED alignment. 7 – Working electrode for axon n1, 8 – Working electrode for axon n2, 9 – Working electrode for axon n3, 10 – Synthetic nerve, 12 – Guide blocks for LEDs (waterproof black cardboard to confine light to each synthetic neuron). **b,** (i) Design of a synthetic nerve. There are seven hydrogel axons encased within an elastomer sheath. The three axons that will be stimulated in patterns are labelled (n1-3). Zoom of a single synthetic axon with sensory (S) and presynaptic (Pre) droplets at each end. (ii) Schematic of the sensory bilayer containing CM-aR3. (iii) Photograph of the sensory bilayer (in the absence of electrodes) containing CM-aR3. Scale bar: 200 μm. **c,** Signal output (steady-state mean ± SD, n = 3 independent synthetic nerves) detected along neurons n1-3 stimulated with different light pulses (15 s, 0.05 Hz, 5 s, 0.1 Hz and 1 s, 0.06 Hz), or in the absence of a bilayer (NB), absence of CM-aR3 (NP) or when illuminated with IR light (IR) or kept in the dark (D).

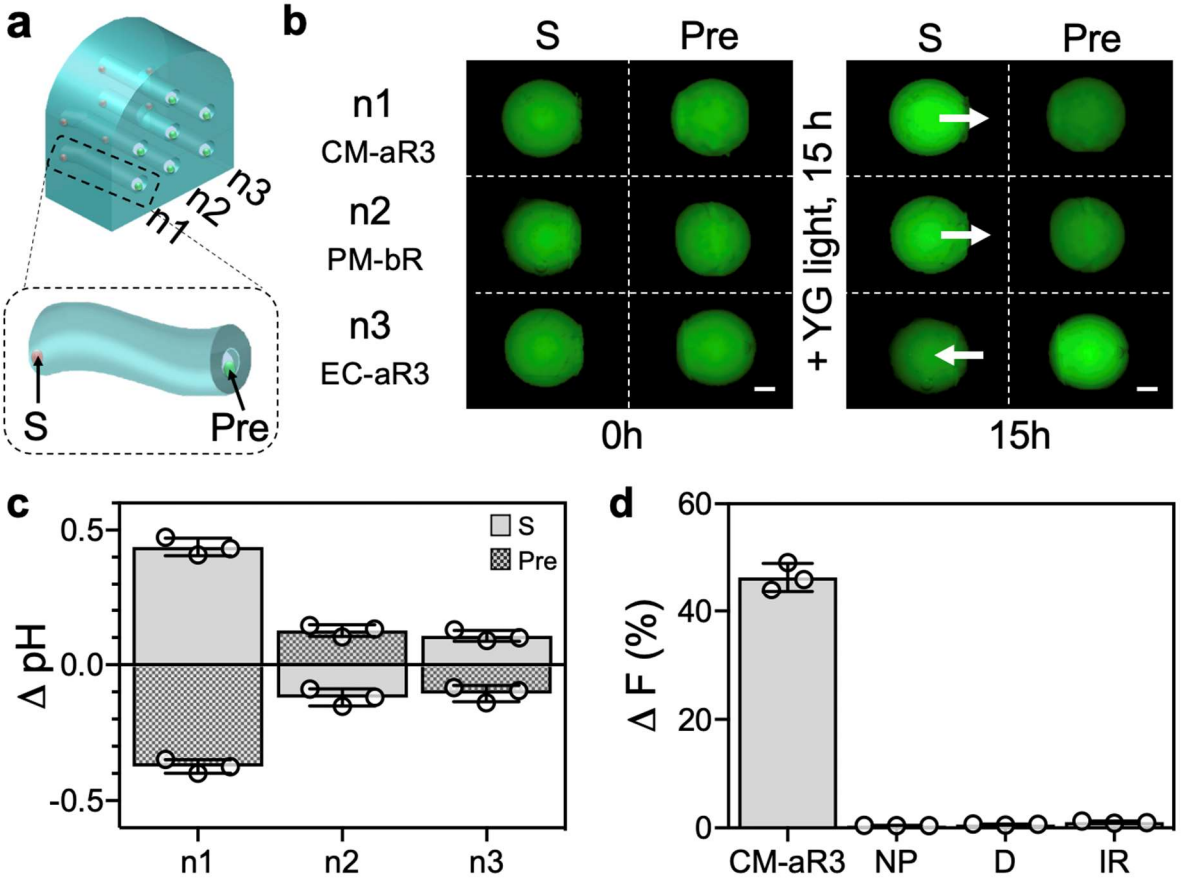

Fig. S26 | Synthetic nerve with patterned sensory droplets. a, Design of a synthetic nerve. There are seven hydrogel axons encased within an elastomer sheath. The three axons that will be stimulated by patterned illumination are labelled (n1-3). Zoom: A hydrogel axon is surrounded with the elastomer sheath. At one end is a sensory droplet (S, + CM-aR3, PM-bR or EC-aR3) and at the other end is a presynaptic droplet (Pre, + αHL). **b,** Sensory droplets are patterned for neurons n1-3 in the synthetic nerve. All droplets contain 100 μM pyranine, 100 mM NaCl, pH 6.5 (in the absence of buffer). The sensory droplets of the neurons contain 0.001% DDM and 0.15 – 0.25 mg mL^{-1} of CM-aR3 (n1), PM-bR (n2) or *E. coli*-expressed aR3 (n3). All presynaptic droplets (Pre) contain 50 nM αHL. Epifluorescence microscopy images (minus background) of the sensory (S) and presynaptic (Pre) droplets are shown before (0 h) and after (15 h) illumination (15 h, YG light, 15 ± 4.5 mW). Arrows indicate direction of H^+ movement across the sensory bilayer. Scale bar = 200 μm. **c,** Changes in pH of the sensory (S, grey) and presynaptic (Pre, grey checked) droplets after illumination for CM-aR3, PM-bR or EC-aR3 (n = 3 independent synthetic nerves, see Materials and Methods)**.** No electrodes were used in these experiments. **d,** Change in fluorescence intensity of the CM-aR3 containing sensory droplet (n1) shown in 'b'. Controls were also performed in the absence of CM-aR3 protein (NP) and when CM-aR3 was illuminated with IR light (IR) or kept in the dark (D).

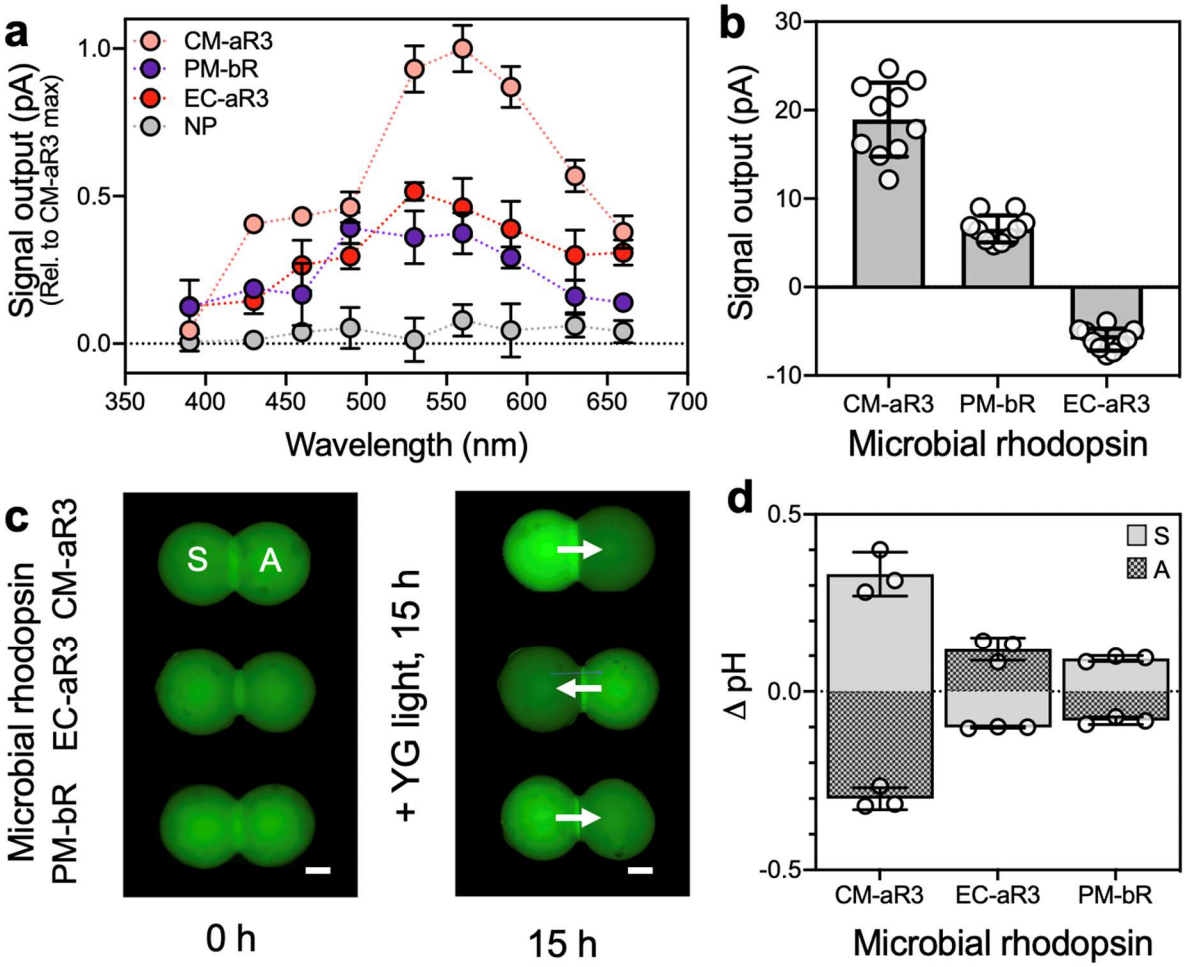

Fig. S27 | Microbial rhodopsin activity. a, Action spectra of the sensory bilayer with CM-aR3 (pink), E. coli aR3 (red), PM-bR (purple), no protein (NP, grey). Signal output is plotted relative to the maximum output of a CM-aR3-containing bilayer (n = 3 independent DIBs). **b,** Signal output recorded across a sensory bilayer containing CM-aR3, PM-bR or EC-aR3 (mean ± SD, n = 10 independent DIBs). CM-aR3 and PM-bR generate positive signals (> 0 pA) whereas EC-aR3 generates negative signals (< 0 pA). **c,** Epifluorescence images (minus background) of a sensory (S) and axon (A) droplet pair containing 100 μM pyranine, 100 mM NaCl, pH 6.5 (in the absence of buffer) illuminated overnight (YG light, 15 h, 15 ± 4.5 mW). Sensory droplets (S) contain 0.001% DDM (w/v) and 0.2 mg mL^{-1} of CM-aR3, PM-bR or *E. coli*-expressed aR3. **d,** Changes in pH of the sensory (grey, S) and axon (grey checked, A) droplets after illumination (n = 3 independent DIBs).

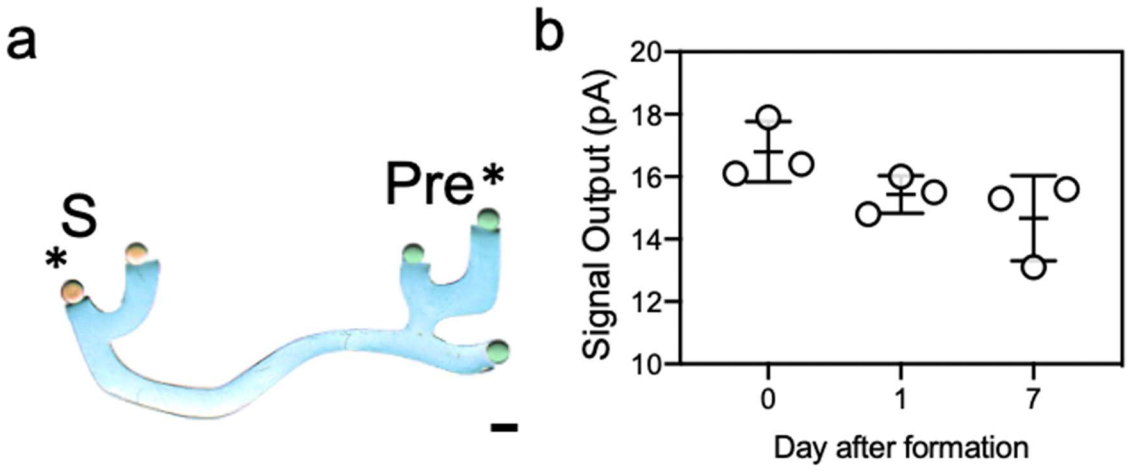

Fig. S28 | Synthetic neuron activity over 1 week. a, Photograph (contains food dye for visualisation, background removed) of a synthetic neuron. Sensory droplet (pink, 100 mM MES, 100 mM NaCl, 0.001% DDM, 0.25 mg mL $^{-1}$ CM-aR3, pH 6.5), axon (blue, 2% agarose, 100 mM NaCl, pH 6.5) and the presynaptic droplet (green, 100 mM NaCl, 50 nM αHL, pH 6.5). Scale bar = 1 mm. **b,** Ag/AgCl electrodes were inserted into the droplets (*) and the signal recorded upon illumination with YG light on day 0, day 1 and day 7 (mean $\pm$ SD, n = 3 independent synthetic neurons). Between recordings, the synthetic neuron is stored in the dark at room temperature, in a hydrated environment.

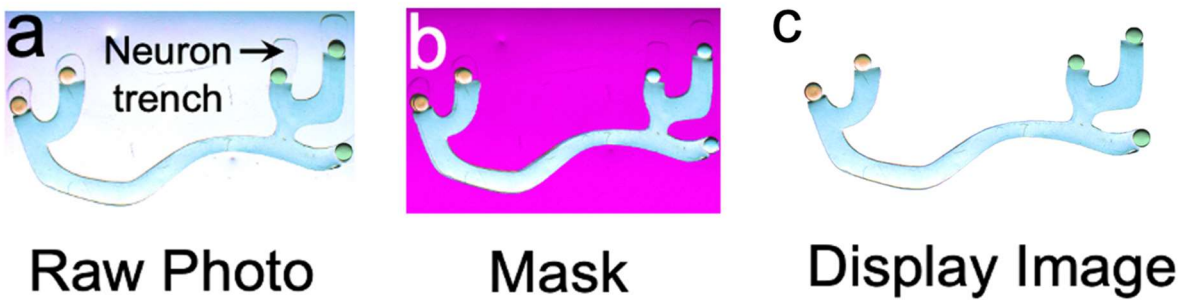

Fig. S29 | Brightfield image processing for display. a, Unprocessed photograph of a synthetic neuron: CM-aR3 droplets (pink, 100 mM MES, 100 mM NaCl, 0.001 % DDM, 0.25 mg mL^{-1} CM-aR3, pH 6.5), hydrogel axon (blue, 100 mM NaCl, pH 6.5, 2% low gelling agarose) and presynaptic droplets (green, 100 mM NaCl, 50 nM αHL, pH 6.5). **b,** Background remove selection on Microsoft PowerPoint highlights the background (pink). **c,** Neuron after background removal generates the display image.

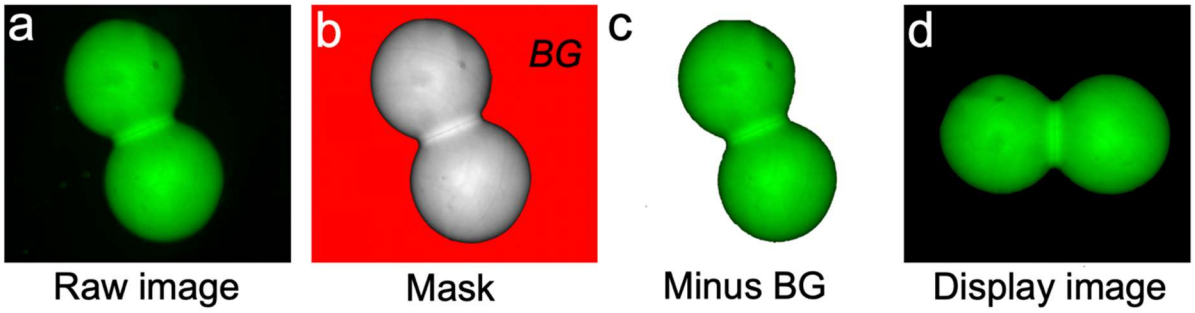

Fig. S30 | Processing of a fluorescence image for display. a, Raw image of a droplet pair containing pyranine (100 μM). **b,** Mask generated using Fiji (ImageJ) highlights the droplet area (grey) marking the background (BG, red). **c,** Droplet pair after mask used to remove background (BG, red in 'b'). **d,** Display image is rotated, and placed over a standard background: this aids visualisation when images are stitched together (see Fig. S12, S30).

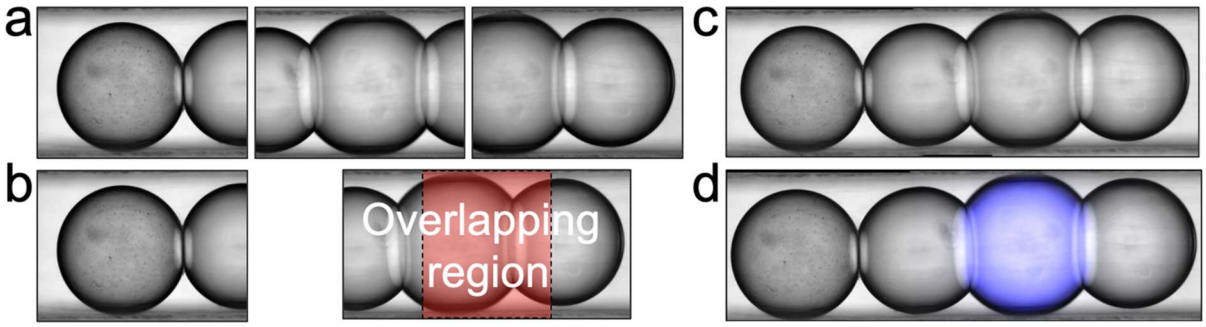

Fig. S31 | Processing of MANT-dATP microscopy images (by stitching) for display. a, Raw, overlapping brightfield images of the synthetic neuron are taken. **b,** Brightfield images are stitched together using the pairwise function in Fiji (ImageJ)[6]. First two of the images are stitched together: the red box highlights their overlapping region. Images are then added onto the stitched image one-by-one until the structure is complete. **c,** Brightfield image of a complete, stitched droplet neuron. **d,** Using the same parameters as the brightfield images, the corresponding fluorescent channels of the droplet neuron are stitched together. The brightfield and fluorescence images of the stitched droplet neuron are overlayed to form the display images.

Supplementary Information: Theoretical Considerations

The signals recorded across the CM-aR3-containing sensory bilayers in our system were below those reported in the literature (when used in alternative systems e.g., in optogenetics)[12,13]. Here, we describe theoretical considerations related to the sensory droplets to provide information concerning the insertion of CM-aR3 into the bilayer within our experimental system (see Materials and Methods). Arguments are adapted from the thesis of Dr Restrepo Schild[3].

1.0 - Dimensions of the CM-aR3 trimer

Proteins from the archaerhodopsin family have been found to pack into trimers in claret membrane patches (CM[12-14]), in a similar manner to the well-characterised hydrogen ion pump, bacteriorhodopsin (bR), which packs into purple membrane patches[15]. The analysis of CM-aR3, including its structure, properties, and proposed mechanism, is ongoing; so we consider values for bR.

According to the structure of bR within the purple membrane (PDB: 2BRD[15]), the trimers of the protein are in a hexagonal unit cell (cross section) with side length (2*a*) of 6.2 nm (2 s.f., a = 3.1 nm). Since the recently deposited structure of CM-aR3 (PDB: 6S6C[13]) overlays closely with the structure of bR, we assume that aR3 in the CM gives the same side length.

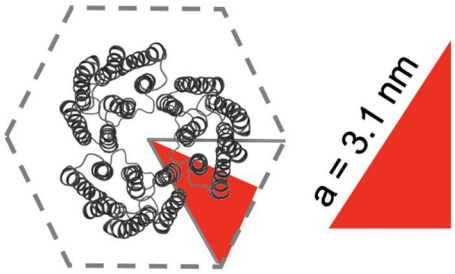

Figure STC1| A hexagonal unit cell of PM-bR. Structure of a bR trimer in purple membrane (PDB: 2BRD[15]) with a hexagonal unit side length of 2a (a = 3.1 nm).

Therefore, the area of a CM-aR3 trimer (A_{aR3}), when packed in the CM, is given by the area of a hexagon with side length 2a:

$$A_{\mathrm{aR3}} = \left(\frac{3\sqrt{3}}{2}\right) \mathrm{a}^2 \quad \text{(E1.0)}$$

which yields an area of ~25 nm^2 (10^{-17} m^2).

– –

2.0 - Quantitation of aR3 in the sensory bilayer

This section aims explores how much CM-aR3 inserts into the sensory bilayer in a functional form.

2.1 Number of aR3 molecules in solution

The number of CM-aR3 trimers (N_{pd}) present in a sensory droplet can be quantified by multiplying Avogadro's constant (N_A, 6.022×10^{23} mol^{-1}), the droplet volume (V_d, L) and, the concentration of protein (C_{pd}, g L^{-1}) over the protein molecular mass (M_p, in units of g mol^{-1}, 27000 g mol^{-1}).

$$N_{\mathrm{pd}} = \frac{C_{\mathrm{pd}}}{M_{\mathrm{p}}} \times V_{\mathrm{d}} \times N_{\mathrm{A}} \quad \text{(E2.0)}$$

For most preparations, within a 200 nL aqueous droplet, there were 10^{11} - 10^{12} aR3 trimers depending upon the aR3 concentration; a typical aR3 concentration of 0.15 – 0.25 mg mL^{-1} was used.

2.2 Ratio of aR3 trimers to DDM micelles

The sensory droplets of our synthetic neurons and nerves contain CM-aR3 at a concentration of 0.15 - 0.25 mg mL^{-1} protein (measured with a nanodrop) in Solution A (100 mM MES, 100 mM NaCl, 0.001% DDM, pH 6.5). Treatment with a low concentration of detergent (DDM), sonication and gently vortexing disrupted aggregation of the crystalline membrane fragments (see Materials and Methods).

The initial step in forming the sensory droplets involves exchanging aR3 into a detergent-containing solution where the detergent is above the critical micelle concentration (CMC, 0.1 % (w/v) DDM). By substituting detergent (N_{dd}) for the number of aR3 molecules (N_{pd}) in Equation 2.0, we determined the number of micelles per aR3 trimer[1] within the sensory droplet (200 nL). The molecular mass used was that of DDM micelles (50000 g mol^{-1})[12] and gives rise to 2^{11} micelles.

$$N_{\mathrm{dd}} = \frac{C_{\mathrm{dd}}}{M_{\mathrm{d}}} \times V_{\mathrm{d}} \times N_{\mathrm{A}} \quad \text{(E2.1)}$$

After sonication, the protein solution is then exchanged into a solution where the detergent is below the critical micelle concentration (CMC, 0.001 % (v/w) DDM, see Materials and Methods).

The free aR3 was calculated as the difference between the number of aR3 trimers (N_{pd}) and the number of detergent micelles (N_{dd}) in the droplet solution. The free aR3 in a sensory droplet is approximately 10^{11} trimers.

$$\text{Free aR3} = N_{pd} - N_{dd} \quad \text{(E2.2)}$$

The aR3 was used at 0.15 – 0.25 g L^{-1}, meaning that there was roughly 10^{-1} – 10^{0} trimers per micelle (when above the critical micelle concentration (CMC), at 0.1 % (w/v)). However, when below the CMC (at 0.01 % (w/v)), this becomes 10^{1} – 10^{2} trimers per detergent molecules, assuming a molecular mass of 510.621 g mol^{-1} (because, as the name implies, there are no micelles when below the CMC).

In our sensory droplets, the aR3 is in CM fragments[1]. We assume that less detergent is required to prevent aggregation of the CM fragments and facilitate their insertion compared to that required for the trimeric and monomeric aR3 (e.g., aR3 expressed in *E. coli*). We observe that if the detergent concentration is not reduced (from 0.1% to 0.001%) then bilayer rupture frequently occurs.

2.3 Bilayer size

Minimum bilayer area to host all available CM-aR3 proteins

Next, we calculated whether the bilayer area (A_{mb}) was large enough to accommodate all the CM-aR3 proteins present in the sensory droplet by using the number of aR3 trimers (N_{pd}, 10^{11} – 10^{12} proteins, Equation 2.0) present in a droplet and the area of a CM-aR3 trimer ($A_{aR3,}$ 10^{-17} m^2, Equation 1.0).

$$A_{mb} = N_{pd} \times A_{aR3} \text{ (E2.3)}$$

Within a 200 nL aqueous droplet there was sufficient protein to cover a surface of 10^{-5} - 10^{-6} m^2.

Area of the experimental CM-aR3 bilayer

Then, we calculated the approximate number of CM-aR3 proteins which could insert into our experimental bilayers. For a single aqueous droplet in the lipid-in-oil solution, the droplet diameter (d_d), is given by:

$$d_d = 2 \times (3\frac{V_d}{4\pi})^{1/3} \text{ (E2.4)}$$

For the 200 nL spherical droplets used in our experimental set-up this gives a droplet diameter (d_d) of ~ 700 μm.

However, within our experimental set-up, the bilayer diameter was only a fraction (f) of the total droplet diameter (d_d) and therefore the bilayer surface area (A_b) was only a fraction (f) of the total droplet cross-sectional area (A_d). We estimate that under our experimental conditions (Materials and Methods), the area of the sensory bilayer is typically between 0.8 and 0.2 (f) of the cross-sectional area of the droplet (Equation 2.4, Fig. SE1, estimated from optical microscopy measurements).

The cross-sectional area of the droplet (A_d) is:

$$A_d = \pi \times (\frac{d_d}{2})^2 \text{ (E2.5)}$$

And the sensory bilayer area (A_b) is:

$$A_b = A_d \times f \text{ (E2.6)}$$

Therefore, the area of the sensory bilayer is between 10^{-7} m^2 (when the bilayer fraction was 80 % of the cross-sectional area, f = 0.8) and 10^{-8} m^2 (when the bilayer fraction was 20 % of the cross-sectional area, f = 0.2) when formed between two 200 nL droplets.

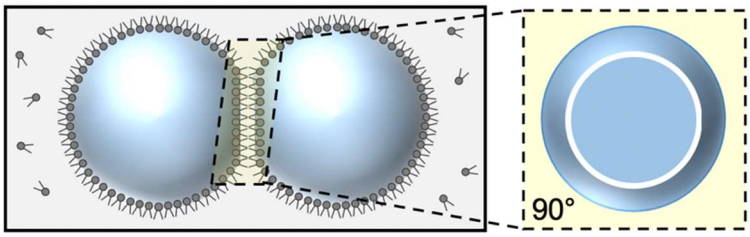

Figure STC2| Area of a bilayer. a, Side view and rotated view (90°) of a DIB with a bilayer which has 80% of the cross-sectional area of the droplet. The white areola represents the edges of the bilayer.

Number of CM-aR3 proteins which fit into the experimental bilayer

By knowing the area of a bilayer (A_b), the maximum number of CM-aR3 proteins which could pack into it (N_{pb}) may be calculated by dividing the bilayer area (A_b) by the CM-aR3 unit area (A_{aR3}, Equation 1.0).

$$N_{pb} = \frac{A_b}{A_{aR3}} \text{ (E2.7)}$$

Therefore, a maximum of 10^9 – 10^{10} (when the bilayer fraction was 20 - 80 % of the cross-sectional area) CM-aR3 trimers could insert into the sensory bilayer formed between two (200 nL) droplets. Since a 200 nL aqueous droplet contains 10^{11} - 10^{12} CM-aR3 trimers (Equation 2.0), there is a large excess of CM-aR3 trimers within a droplet.

2.4 Signal output generated by CM-aR3

Our experimental data, obtained by illuminating the CM-aR3-containing sensory bilayer with yellow-green light, gave signals of ~10^1 pA (lower than reported elsewhere in the literature, where several hundred to thousand picoamps have been generated[13,16]).

The signal (in a tethered droplet network, with Ag/AgCl electrodes) is the product of the electron charge (1.6×10^{-19} C, the electrodes convert the ionic current to electrons**)**, the charge of the ionic species pumped (+1 for hydrogen ions), the rate of the limiting step in the CM-aR3 photocycle (k_p, ~20 H^+ s^{-1})[16] and the number of CM-aR3 trimers in the bilayer (N_{pb}, Equation 2.7, 10^{11} – 10^{12} CM-aR3 trimers).

$$I_{max} = N_{pb} \times 1.6x10^{-19} \times 1 \times k_p \text{ (E2.9)}$$

The net number of aR3 proteins that insert N-terminus first into the sensory bilayer (N_n) equals the quotient of the transport rate of electrons (in the external circuit, $e^- t^{-1}$) and the photocycle rate of aR3 (k_p, ~20 H^+ s^{-1})[16].

$$N_n = \frac{e^-/t}{k_p} \text{ (E2.10)}$$

Based on a recorded signal of +15 – 25 pA for CM-aR3 we determine that there is a net number of 10^5 - 10^6 proteins inserted N-terminus first (i.e. pumping hydrogen ions out of the sensory droplet) in the bilayer (from a maximum of 10^9 – 10^{10} CM-aR3 trimers that could insert from solution and when the bilayer fraction was 20 - 80 % of the cross-sectional area).

2.5 Hydrogen ion pumping limitations

This current output begs the question of how long it will take until no more hydrogen ions (H^+) can be pumped out of the sensory droplet. Two factors will limit H^+ pumping: the number of H^+ available in the sensory droplet and the time taken for a pH gradient to form that inhibits aR3 activity. Whilst aR3 can pump H^+ against a concentration gradient, the formation of a pH gradient (>1 pH unit) hinders pumping[3,14]. The presence of a buffering agent (MES) in the sensory droplet and the ability of ions to move down the axon and away from the sensory droplet prevent a large pH gradient from rapidly building up.

2.6 Summary of possible reasons for low H^+ pumping rates

There are several reasons why a signal 2-5 orders of magnitude lower than those reported in the literature[12,13] was generated in our experimental system (Materials and Methods):

1. **Bilayer size**:

Perhaps, the bilayer is much smaller than 20% of the cross-sectional area of the droplets meaning fewer CM-aR3 proteins can insert into it. However, if we assume that the bilayer is packed with protein and those proteins pump at their maximum rate ($k_p = 10^0 - 10^2$)[17], then the bilayer area would have to be 0.000001% of the droplet cross-section. We know that this is not the case from optical microscopy measurements (since the bilayer can be easily observed as larger than this), so bilayer size is unlikely to the main limitation.

2. **Photokinetics and stability**

Perhaps the activity of the CM-aR3 is reduced by the reconstitution procedure. The detergent treatment of CM-aR3 and the use of the unnatural DPhPC as the bilayer lipid might disturb the photokinetics and protein stability. However, for this to be sole cause, the photocycle rate would have to be reduced five-hundred-fold (reported rate $k_p = 10^0 - 10^2$)[17], in a fully packed membrane under our experimental light-saturating conditions.

3. **Orientation**

CM-aR3 is purified as fragments of the claret membrane (see Materials and Methods). Such fragments might insert into the bilayer randomly or with only a slight preference for a particular orientation. Research has shown that the addition of hydrophilic moieties aided directional insertion of microbial rhodopsins into artificial bilayers[19]. However, in our system, protein translocation rates remained low when a hydrophilic extension was fused to one end of the microbial rhodopsin forcing a single orientation (unpublished)[3].

4. **Inefficient insertion**

Unsurprisingly, the most likely reason for low H^+-pumping activity is inefficient functional insertion of CM-aR3 into the bilayer. It might be that the membranes (CM fragments or vesicles) fail to insert or are semi-fusing (i.e., not entirely merging together), forming a convex arrangement that alters the bilayer topology and makes it less favourable for an additional fragment insertion. Another explanation might be that the DPhPC bilayer requires a certain

distance between patches or proteins (perhaps due to tensile stress – the patches/proteins exert a force on the bilayer) and therefore tight packing cannot take place.

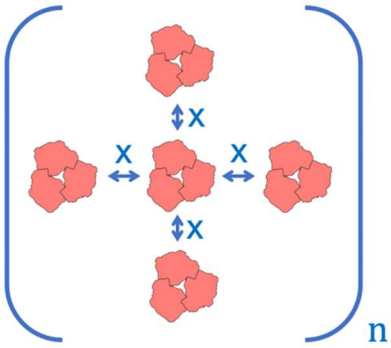

Fig. STC3 | The bilayer may require a set distance between patches or proteins. Schematic, top view of a bilayer with proteins inserted at a set distance (x) from each other.

Supplementary Information: References

1. Bada Juarez, J.F., Judge, P.J., Adam, S., *et. al.* Structures of the archaerhodopsin-3 transporter reveal that disordering of internal water networks underpins receptor sensitization. *Nat. Commun.* **12,** 629 (2021).
2. Cline, S. W., and Doolittle, W.F. Efficient transfection of the archaebacterium Halobacterium halobium. *J. Bacteriology.* **163,** 1341-1344. (1987).
3. Restrepo Schild, V. Light-activated synthetic tissues. [PhD Thesis]. University of Oxford. (2020).
4. Orwick-Rydmark, M., Lovett, J. E., Graziadei, A., *et. al.* Detergent-free incorporation of a seven-transmembrane receptor protein into nanosized bilayer lipodisq particles for functional and biophysical studies. *Nano. Letters.* **12,** 4687-4692. (2012).
5. Ming, M., et. al. pH dependence of light-driven proton pumping by an archaerhodopsin from Tibet: comparison with bacteriorhodopsin. *Biophys. J.* **90**, 3322-3332. (2006).
6. Preibisch, S., Saalfeld, S., & Tomancak, P. Globally optimal stitching of tiled 3D microscopic image acquisitions. *Bioinformatics.* **25**(11), 1463-1465 (2009).
7. Bean, B. P. The action potential in mammalian central neurons. *Nat. Rev. Neurosci*. **8**, 451–465 (2007).
8. Lodish, H., et. al. Molecular Cell Biology. (W.H. Freeman, 2016).
9. Hodgkin, A. L., and Huxley, A. F. A quantitative description of membrane current and its application to conduction and excitation in nerve. *J. Physiol.* **117,** 500-544. (1952).
10. Pundir, S., Martin, M.J., O'Donovan, C., and the UniProt Consortium. UniProt Tools. *Curr. Protoc. Bioinformatics.* **53,** 1.29.1-1.29.15. (2016).
11. Ihlenfeldt, W.D., Bolton, E.E.,and Bryant, S.H. The PubChem chemical structure sketcher. *J. Cheminform.* **1,** 20 (2009).
12. Ernst, O. P., Lodowski, D.T., Elstner, M. et. al. Microbial and animal rhodopsins: structures, functions and molecular mechanisms. *Chem. Rev*. **8**, 126-163 (2014).
13. Chow, B.Y., Han, X., Dobry, A.S., *et. al.* High-performance genetically targetable optical neural silencing by light-driven proton pumps. *Nature.* **463,** 98-102. (2010).
14. Henderson, R., and Grigorieff, N. Crystal structure of bacteriorhodopsin in purple membrane. doi: 10.2210/pdb/BRD/pdb. (1996).
15. *n-Dodecyl β-D-maltoside.* Merck (Sigma). Accessed 19th March 2020. [https://www.sigmaaldrich.com/catalog/product/sigma/d4641?lang=en&region=GB].
16. Inoue, K. et al. Converting a light-driven proton pump into a light-gated proton channel. *J. Am. Chem. Soc*. **137**, 3291-3299 (2015).
17. Huang, K-S., Bayley, H., and Gobind Khorana, H. Delipidation of bacteriorhodopsin and reconstitution with exogenous phospholipid. *Proc. Nat. Acad. Sci.* **77,** 323-327. (1980).
18. Ritzmann, N., Thoma, J., Hirschi, S., *et. al*. Fusion domains guide the oriented insertion of light-driven proton pumps into liposomes. *Biophys. J.* **133(6):** 1181-1186. (2017).